International Journal of Earth Sciences (2021) 110:1049–1071
https://doi.org/10.1007/s00531-021-02006-y

ORIGINAL PAPER

Petrographical and mineralogical study of detrital strata near and within the Ballık travertine deposit (SW Turkey): architecture of a mixed clastic–carbonate succession

Michaël Verbiest[1] · Jeroen Soete[2] · Ophélie Fay-Gomord[1] · Rieko Adriaens[3] · Cihan Aratman[1,4] · Rudy Swennen[1]

Received: 24 July 2020 / Accepted: 5 February 2021 / Published online: 29 March 2021

Abstract
The Ballık area (SW Turkey) was studied as a mixed clastic–continental carbonate reservoir analogue, in which kilometre wide and up to 70-m-thick tufa and travertine lithologies are found in an envelope of detrital sediments, which locally strongly interfinger with these porous carbonates. Former studies focussed on the carbonate lithologies, since they are considered as pre-salt analogues. This study aims to describe the adjacent non-carbonate lithologies, unravel their depositional setting, and address their influence on the overall sedimentary architecture. This study relies on an extensive field campaign, during which 142 samples of all different detrital lithologies were collected. Optical, fluorescence, cathodoluminescence, and Scanning Electron Microscopy (SEM) yielded important insights in the petrography of these lithologies, based on which 5 main lithologies were differentiated: i.e., (1) laminated marls, (2) polygenetic conglomerates, (3) massive marls, (4) tabular sandstones, and (5) coquina accumulations. These were interpreted to represent three different sedimentary facies corresponding to lacustrine, fluvial, and shoreline facies. The (clay) mineralogy of lacustrine sediments was extensively studied by bulk and clay-specific XRD. In this respect, special emphasis was laid on the depositional setting of the lacustrine facies, in which both authigenic palygorskite and poorly ordered dolomite were identified. Petrophysical properties of 16 plugs were determined by He porosimetry and N2-permeability, indicating that the detrital sediments are characterised by poor reservoir properties. The latter causes them to act, after assumed burial compaction, as potential barriers within a continental carbonate reservoir system.

Keywords Palygorskite · Varves · Clastic sediments · Conglomerate · Carbonate sediments · Mixed carbonate–clastic system

Introduction

The discovery of the Pre-Salt play in the South-Atlantic has sparked interest in reservoir properties of continental carbonate systems worldwide, which often are mixed with clastic sediments. 5–8 Billion Barrels of Oil Equivalent (BBOE) have been estimated to be in place in the Pre-Salt reservoir located in the Tupi area, highlighting the economic importance and the need to acquire detailed knowledge about these new reservoir systems (Beltrão et al. 2009). The Pre-Salt reservoirs tend to develop in a wide range of depositional settings, ranging from continental to sub-aqueous environments, leading to complex reservoir architectures (Virgone et al. 2013). In the specific case of the Lula-field, which is dominantly made of (microbial) continental carbonates, siliciclastic beds and coquina layers have been encountered (Muniz and Bosence 2015).

✉ Michaël Verbiest
michaelverbiest@msn.com

[1] Division of Geology–Department of Earth and Environmental Sciences, KU Leuven, Celestijnenlaan 200E, 3001 Leuven-Heverlee, Belgium

[2] Department of Materials Engineering–Structural Composites and Alloys, Integrity and Nondestructive Testing, KU Leuven, Kasteelpark Arenberg 44, 3001 Leuven-Heverlee, Belgium

[3] QMineral, Analysis and Consulting, Gaston Geenslaan 1, 3001 Leuven-Heverlee, Belgium

[4] Department of Geological Engineering, Pamukkale University, Kınıklı Campus, 20070 Denizli, Turkey

The mixed clastic–continental carbonates of the Ballık area, located east of Denizli, are a well-documented sub-seismic sized, analogue system of sub-aqueous as well as domal travertines (e.g., Özkul et al. 2013; Claes et al. 2015; Desouky et al. 2015; Soete et al. 2015; Van Noten et al. 2019). Two noteworthy complementary studies in the Ballık area, addressing the depositional setting and palaeoclimatic evolution of an adjacent Middle-to-Late Pleistocene travertine body and the Pleistocene paleoenvironment, were presented by Toker et al. (2015) and Rausch et al. (2019), respectively. The former studies mainly focussed on the sedimentological and petrophysical characteristics of the porous continental travertines. However, as already mentioned by Claes et al. (2015), clastic facies occur adjacent to and intercalated within the travertines. The mixed clastic–carbonate system of the Ballık travertine dome thus provides a great opportunity to assess the effects of clastic sediments on the architecture of a continental carbonate analogue. To understand the effects these clastic sediments have on the reservoir analogue, petrographic and sedimentary observations on these sediments must be taken into account.

Claes et al. (2015) already concluded that the clastics, i.e., marls and conglomerates, represent a shallow lacustrine-dominated depositional system combined with the presence of fluvial channels. The occurrence of clastic intervals, especially when containing clays and being interlayered with porous continental carbonate layers, might lead to compartmentalisation of the reservoir, with implications for reservoir modelling. Since these detrital sediments represent key features in the well-exposed Ballık analogue, their properties are essential to improve our understanding of the extent that detrital sediments might influence reservoir architecture. In addition, the transition from a carbonate towards a detrital dominated system reflects an important change in the depositional setting. Therefore, this study aims to develop a facies classification for the clastics, which occur adjacent to and as intercalations within the continental carbonates. This classification will improve the understanding of their sedimentological characteristics and origin, and will help to acquire a better insight into their distribution throughout the reservoir analogue, whilst taking into account their reservoir characteristics.

Geological setting

The studied deposits in the Ballık area are located east of Denizli, in the south-western part of Turkey, at the junction of the Çürüksu and Baklan grabens (Van Noten et al. 2013). Since the emphasis of this paper lies with the detrital sediments surrounding the Ballık travertine dome, the overall geological setting will only be briefly discussed. For further understanding of the regional geology in south-western Turkey and the graben configuration, the reader is referred to the studies by Bozkurt (2001, 2003) and ten Veen et al. (2009), while the studies of Alçiçek et al. (2013) and Van Noten et al. (2019) focus on the geological setting around and within the Ballık study area.

The Ballık area is situated on the northern flank of the Denizli Basin, which is bound by major escarpments that are interpreted as footwalls of a succession of normal faults, resulting from the N–S-oriented tectonic extension (Westaway et al. 2005; Alçiçek et al. 2019). The detrital sediments discussed in this paper are presented in different quarries (Fig. 1). All these quarries are located in the so-called lower domal area (Van Noten et al. 2013).

The potential provenance area of the detrital sediments, studied in this paper, corresponds to 4 different geological units, visualised in Fig. 2 (compiled after Capezzuoli et al. 2018; Van Noten et al. 2019 and the Geological Survey of Turkey). The Menderes massif (1), composed of Pre-Cambrian-to-Early Paleozoic strata has undergone a Barrovian-type metamorphism and crops out west of the study area. This massif is composed of a succession of augen-gneiss, metagranite, migmatite, gabbro, and medium- to high-grade metamorphic schists. The second unit, namely the Lycian Nappes (2), is Triassic–Jurassic in age and is exposed north and east of the study area. They consist of meta-siliciclastic sediments, limestone, and evaporitic dolomite (Alçiçek et al. 2019). The last units, including the dominantly Neogene Denizli Group (3) and the Quaternary strata (4), are composed of a combination of alluvial fan, delta, shallow marine, and lacustrine sediments (Alçiçek et al. 2019).

The studied detrital sediments are spatially closely associated with the Ballık travertines, which formed by carbonate precipitation that started max. 1.78 Ma ago and ceased at least 1.1 Ma ago (Lebatard et al. 2014). The overall continental carbonate analogue was studied by Claes et al. (2015), who reported aggradational sub-horizontal travertine facies, deposited in a sub-aqueous setting, in the lower part of the carbonate succession. Within this succession, he noticed the presence of clastic intercalations and flanking strata. Vertically, this sub-horizontal facies is succeeded by the so-called domal structure yielding irregular slope deposits. Claes et al. (2015) concluded that the succession of travertine facies is related to the changing flow path of down-flowing water, controlling where and how fast, calcite precipitation takes place. Rausch et al. (2019) studied the paleoenvironment in the Denizli basin, integrating micro- and macro-paleontological species, such as ostracods, molluscs, decapod crustacean, vertebrate relics, leaf imprints, and relicts of *Homo erectus*.

More in detail, the reservoir analogue system consists of 6 different major sedimentological units, either dominated by continental carbonates (C) or detrital (D) sediments (Fig. 3). The emphasis of this study lies in the description

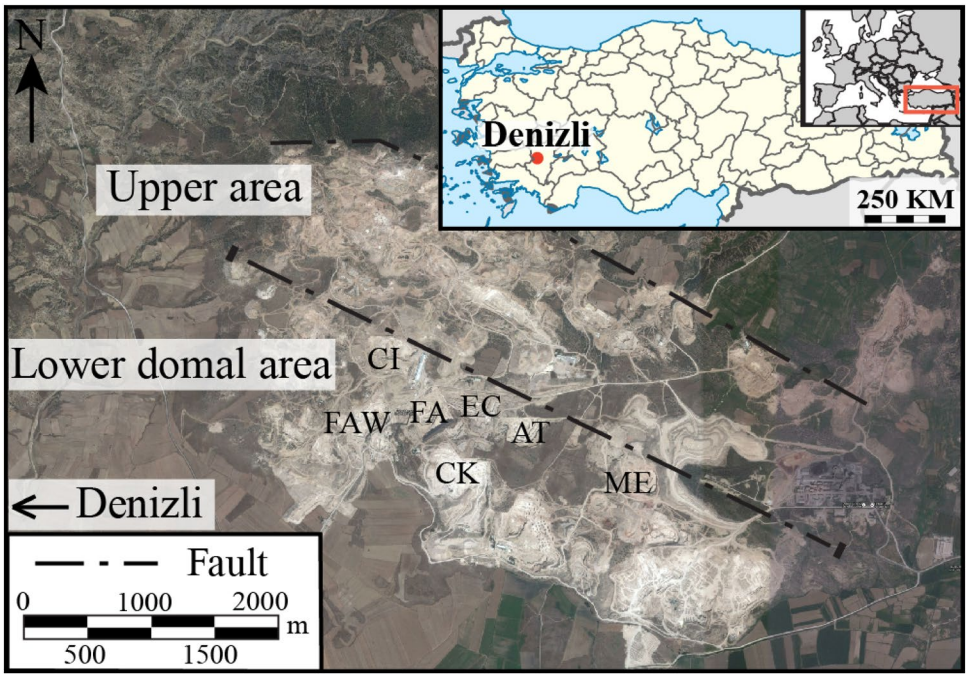

Fig. 1 Study area, with indication of the studied quarries in the so-called lower domal area (Alimoğlu-Tasarim, AT; Çakmak, CK; Cinkaye, CI; ECE, EC; Faber, FA; Faber West, FAW and Metamar, ME)

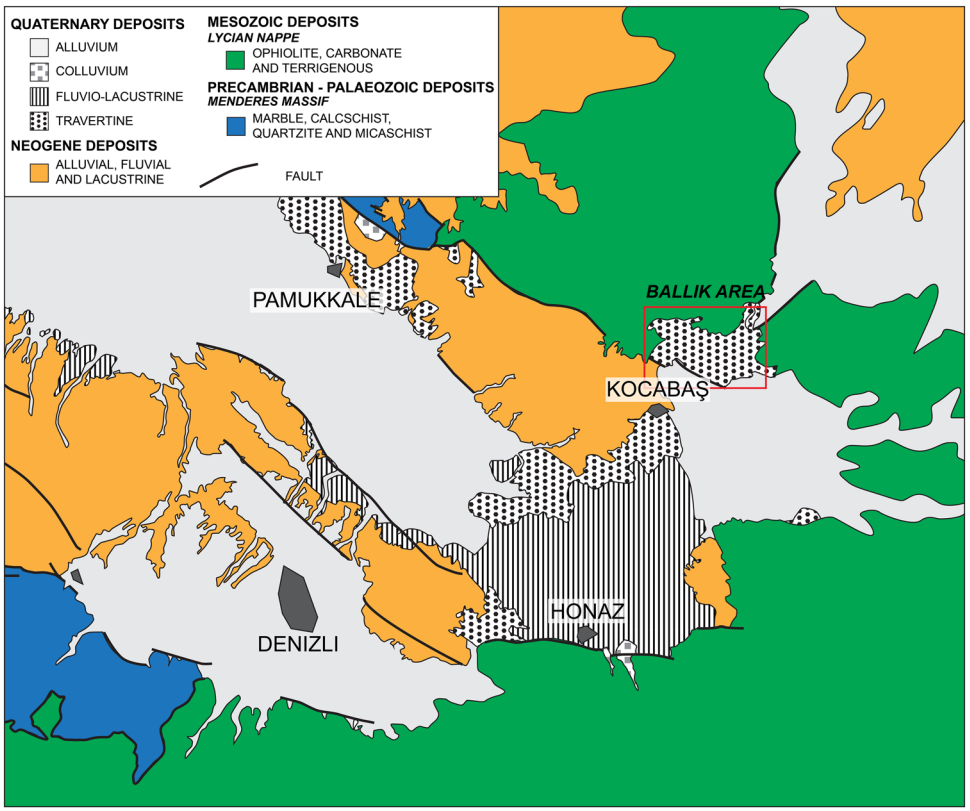

Fig. 2 Simplified geological map of the region surrounding the Ballık area, highlighting the five major geological units surrounding the studied analogue (compiled after Capezzuoli et al. 2018; Van Noten et al. 2019 and the Geological Survey of Turkey)

of the detrital sediments and the way they are part of the architecture of the mixed clastic–carbonate succession. Claes et al. (2015) focussed more on the carbonates and described the basal sequence as aggradational sub-horizontal travertines, deposited in a sub-aqueous environment (Fig. 3, C1; lower travertines of Rausch et al. 2019). The oldest clastic deposit is a rather local phenomenon and is encased within the sequence of sub-horizontal travertines (Fig. 3, D1). The second detrital sequence forms a wedge (Fig. 3, D2; lower conglomerates of Rausch et al. 2019)

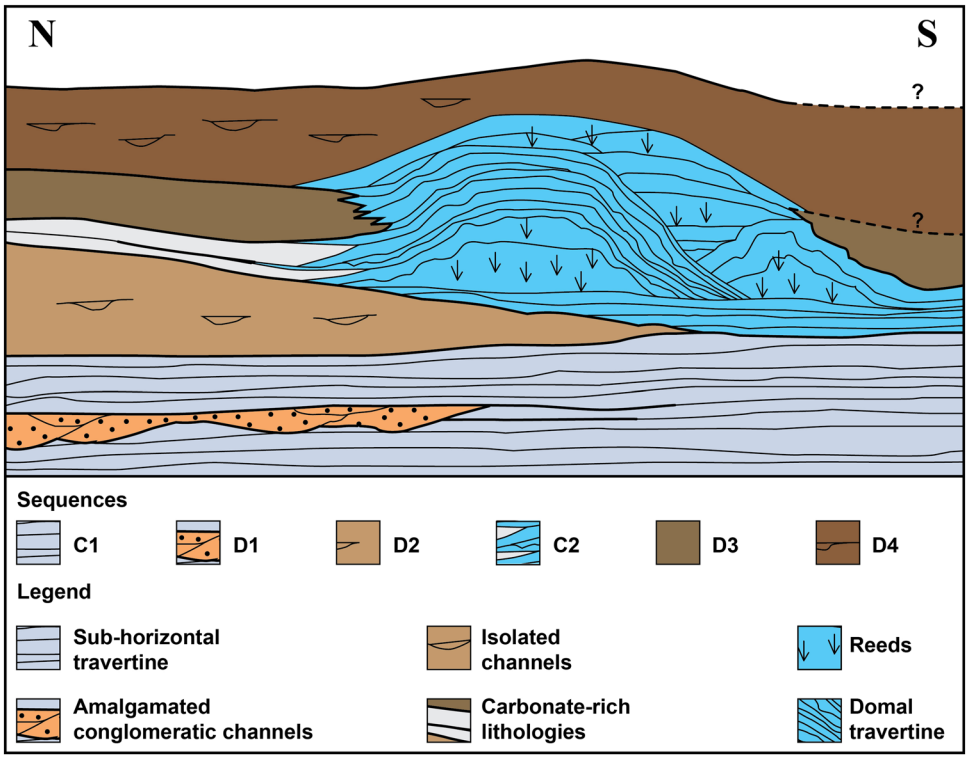

Fig. 3 Simplified architectural model of the Ballık reservoir analogue system, highlighting the presence of six sedimentary sequences. The top surface of sequence C2 is not horizontal, but exhibits a domal shape. The latter is a consequence of the development of subaerial travertines, as well as the differential compaction of travertine and the surrounding and overlying siliciclastic lithologies

near the boundary of the sub-horizontal and domal travertine sediments, pinching out towards the South East. This sequence is initially characterised by fluvial deposits (conglomerates), while the centre of this sequence is characterised by lacustrine deposits (laminated marls). The deposits near the top of this sequence are again fluvial, consisting of a mixture of conglomerates and massive marls. These deposits are covered by domal travertine sediments that are initially characterised by sub-horizontal travertine lithologies and evolve towards domal structures due to the stabilisation of the carbonate mounds by reeds (Fig. 3, C2; upper travertines of Rausch et al. 2019). The latter allows slopes to develop, leading to cascade and eventually waterfall travertine lithologies. Contemporaneous with this sequence of domal travertine, the deposition of carbonate-rich detrital lithologies is observed adjacent to the domal carbonate structure (Fig. 3, white equivalent of C2). The latter is topped by the third detrital sequence, which intertwines with the adjacent domal travertine lithologies (Fig. 3, D3 upper conglomerates of Rausch et al. 2019). It is in these domal travertines (C2) and conglomerates (D3) where Rausch et al. (2019) discovered most fossils. The latter authors concluded that there existed a mixed landscape (shrubby, arboreous, and near-water vegetation to a savannah-like landscape), which formed under temperate and humid climatic conditions. The fourth and final detrital sequence (Fig. 3, D4) occurs both adjacent to and on top of the domal travertine lithologies and was not reported by Rausch et al. (2019), since they are poorly preserved in their studied section of the Ballık travertine dome.

Materials and methods

Sampling and logging

Seventeen lithologs were made to create a log correlation of the different lithologies throughout the study area. The latter provides information regarding the distribution of different lithologies both laterally and vertically. 142 samples were acquired, spread throughout 7 different quarries of the Ballık area, representing all different detrital lithologies. 35 of these samples were selected for detailed petrographical and petrophysical analysis, while the others were described as hand specimens. Well-cemented lithologies were sampled as horizontal plugs, with a diameter of 2. 54 cm and a length of 5 cm, while poorly cemented lithologies were sampled as hand-specimen.

Petrography and mineralogy

Thirty-five thin sections were prepared and impregnated with a fluorescent epoxy resin. Thin sections were described using optical light and fluorescence microscopy on an Olympus BX41, connected to a fluorescent light source of Leica

(12 V/100 W-type). Cold cathodoluminescence analyses were performed to study the varying chemical composition of carbonate cements, using a modified Techosyn Model 8200 Mark II.

Due to the macroscopic scale of certain sedimentary structures, thin-section scans taken both under parallel and crossed polars were acquired at a resolution of 1200 DPI with an EPSON transmitting light scanner. Image analysis was performed at several scales (cf. upscaling) of all thin sections with the software package of JMicrovision (V. 1. 3. 2, Roduit 2007). 2D porosity was determined using either point-counting (user-controlled) or object extraction (colour-threshold controlled).

Furthermore, 10 samples were studied by Scanning Electron Microscopy (SEM) to identify the authigenic minerals present in the sediments. Analyses were carried out by two different instruments, a JEOL JSM 6400 Scanning Microscope (magnification from 1000 to 5000 times) and an EM XL30 FEG Field Emission Microscope (magnification from 1000 to 20,000 times). Both devices were equipped with an Energy-Dispersive Spectrometer (EDS) and mineral identification was based on the SEM petrology atlas of Welton (1984).

The mineralogical composition of the marl lithologies was assessed trough both bulk ($n = 8$) and clay-specific ($n = 6$) X-Ray Diffraction (XRD). Bulk powder analysis was used to quantify the overall mineralogical composition. These measurements were performed with a PW1050/37 goniometer in a Bragg–Brentano θ/2θ setup, which was connected to a PW1830 generator equipped with a Cu-Kα-radiation source and a proportional detector type PW3011/00. Bulk powders of each sample were measured with the following XRD settings: 1h40 measurement duration, 0. 02° 2θ step size, 2 s counting time per step over a 5°–65° 2θ range. To study the specific clay mineralogy, the samples underwent selective chemical treatment, which removed carbonate cements, organic matter, and Fe-(hydro) oxides (modified after Jackson 1973). The < 2 µm fraction was extracted using timed centrifugation, resulting in a purified clay fraction that was used to prepare oriented clay preparation by the sedimentation technique (Moore and Reynolds 1997). The same device as for the bulk measurements was used, but with the following measurement settings: 0h38 measurement duration, 0. 02° 2θ step size, 1 s counting time per step over a 2°–47° 2θ range. Samples were characterised, based on both ethylene–glycol saturated and air-dried clay slides, to distinguish different clay minerals.

Petrophysical characterisation

Helium porosity and Klinkenberg corrected horizontal permeability of 16 plugs, with a diameter of 1 inch, were assessed by PanTerra Geoconsultants. Porosity was measured with a helium expansion porosimeter, allowing to determine the effective porosity of each plug. Horizontal gas permeability was determined with a Vinci nitrogen permeameter, in which plugs where mounted in a Hassler core holder at a pressure of 400 psi (simulating reservoir conditions). Gas slippage was accounted for by correcting the measured permeabilities based on Klinkenberg's empirical correlation.

Due to the unconsolidated state of certain lithologies (e.g., laminated marls), He-porosity or N2-permeability measurements could not be performed. Therefore, 2D porosity was estimated in JMicroVision through image analysis at several scales, whilst following an upscaling methodology and considering the required representative elementary volume as described by Bear (1972).

Results

Sedimentary architecture

The Quaternary deposits in the Ballık area are characterised by the presence of both continental carbonates and clastic lithologies and can thus be classified as a mixed travertine-terrigenous system. Similar depositional systems were described by Croci et al. (2016) (Tuscany, Central Italy) and Mors et al. (2019) (Catmarca, Argentina). Previously, Claes et al. (2015) observed the presence of three different marl-to-marl–conglomeratic sequences in some of the most representative quarries of Ece and Faber (Fig. 1), located in the northwestern part of the Ballık area. During this study, a fourth detrital sequence was observed in the southeastern part of the Ballık area (exposed in the quarries of Alimoğlu-Tasarim and Çakmak; Fig. 1). In the section below, first, the sedimentary sequence is addressed before the different observed lithologies will be described.

Detrital sequences

Detrital unit D1 has a max. thickness of 6 m and was solely observed in the Faber quarry, while the other three detrital sequences (D2, D3, and D4) were outcropping all over the Ballık area. D1 differs from the other three sequences in its lateral extent and depositional build-up. In contrast to the other sequences, this unit solely consists of an alternation of both travertines, enriched in detrital grains and polygenetic conglomeratic beds. The latter consist of well-rounded clasts with a diameter of 0. 5 up to 20 cm and their thickness varies between 0. 2 and 0. 6 m. Larger clasts have a more angular shape and are dominantly made of layered lithologies similar to the surrounding sub-horizontal travertine. In general, the conglomeratic beds are characterised by their erosive nature and are fining upwards. These beds are amalgamated and

their fabric is dominantly grain-supported, with the exception of the upper part which is mud-supported (Fig. 4a, b). In addition, imbricated structures were observed, indicating a paleo-current oriented towards the south (Fig. 4c).

Since all other detrital sequences were observed in two or more quarries, a simplified log correlation is presented in Fig. 5. In general, the western part of the Ballık area is better exposed than the eastern side, leading to fewer outcrops in the east. Therefore, the eastern section is under-represented in the reported observations. The second detrital sequence was observed in the quarries of Çakmak, Faber, and Faber West, and lies on top of so-called sub-horizontal travertines (Claes et al. 2015). The thickness of this sequence is estimated at about 11 m in Faber West, decreasing continuously to 5 m in the eastern-most section of the Faber quarry, thus displaying a wedge-shaped geometry. Proximal to the Ballık travertine dome, in the quarries of Faber and Çakmak, this sequence is topped by an intercalation of cascade travertines. In the distally located quarry of Faber West, this intercalation is gradually replaced by carbonate-cemented marls, thickening westwards (Fig. 5). In general, the base of this sequence consists dominantly of fining upward conglomeratic beds with decreasing erosive nature at a greater distance from the Ballık travertine dome (west), as reflected by decreasing clast size. Root traces, highlighted by manganese oxides, were often observed at the top of these conglomeratic beds. Conglomeratic channels become less abundant towards the middle of this sequence, where fine-grained lithologies more frequently occur. In the distal areas, away from the Ballık travertine dome, this leads to the deposition of massive marls, while laminated marls are abundantly present in more proximal areas. Grain-supported, multi-channel, and erosive conglomeratic beds are dominant in the upper part of this sequence. Proximal to the Ballık travertine dome, these conglomerates are observed to be floating in a travertine matrix with moulds of reed stems.

The third detrital sequence has a thickness of about 8 m and covers most of the quarries in the western part of the Ballık area. In the quarries of Çakmak and Faber, this sequence is observed on top of cascade travertines, while it covers carbonate-rich marls in Faber West. The occurrence of these detritals along the flanks of the Ballık travertine dome indicates that the build-up of the travertine dome was already active prior to the deposition of this sequence. The third sequence consists of an alternation of laminated marls and conglomeratic beds, with significant heterogeneities between locations. Adjacent to the travertine dome, both in Çakmak and in Faber, thinning wedges of laminated marls were observed, restricted in geometry by the topography of domal travertine deposits. The transition between

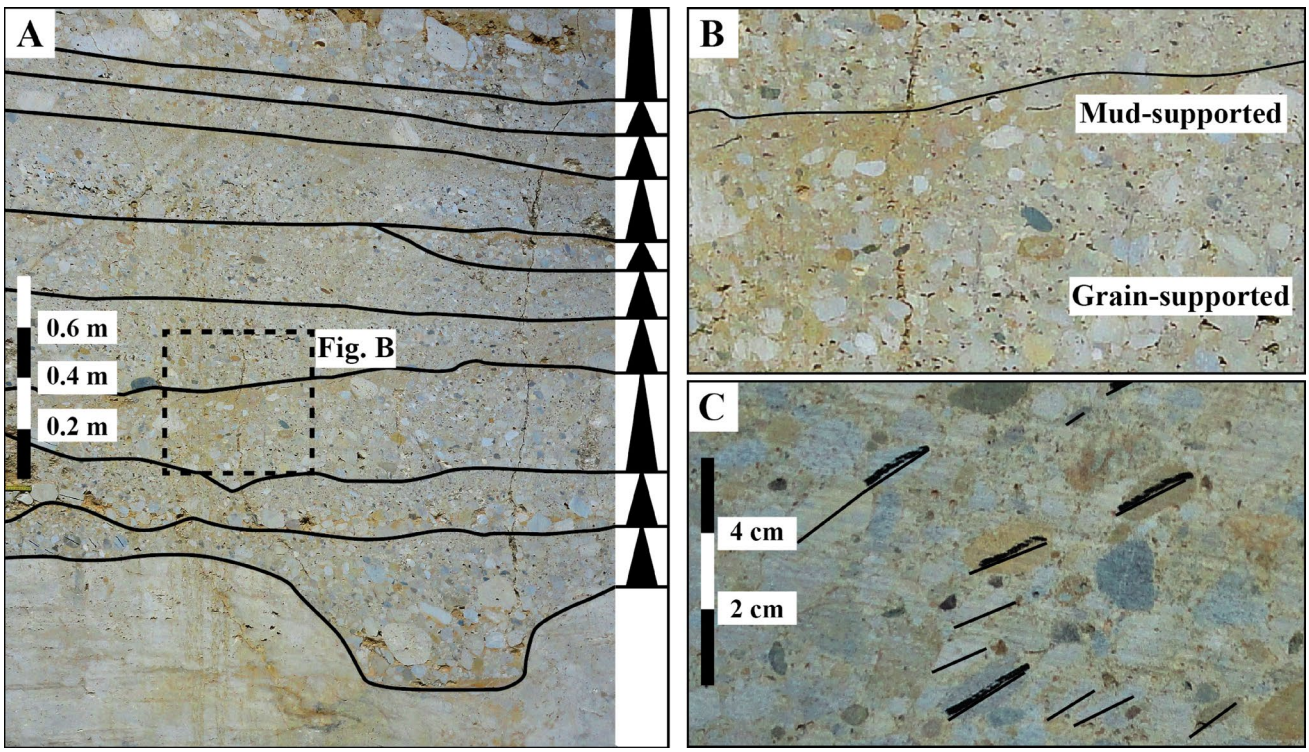

Fig. 4 Macroscopic and microscopic observations of polygenetic conglomerates. **a** Outcrop of amalgamated conglomeratic beds, with fining upwards structures (black triangles) and erosive contacts (black lines). **b** Texture of conglomeratic beds evolves from grain-supported to mud-supported towards the top. **c** Imbrication structures indicating a paleo-current towards the south

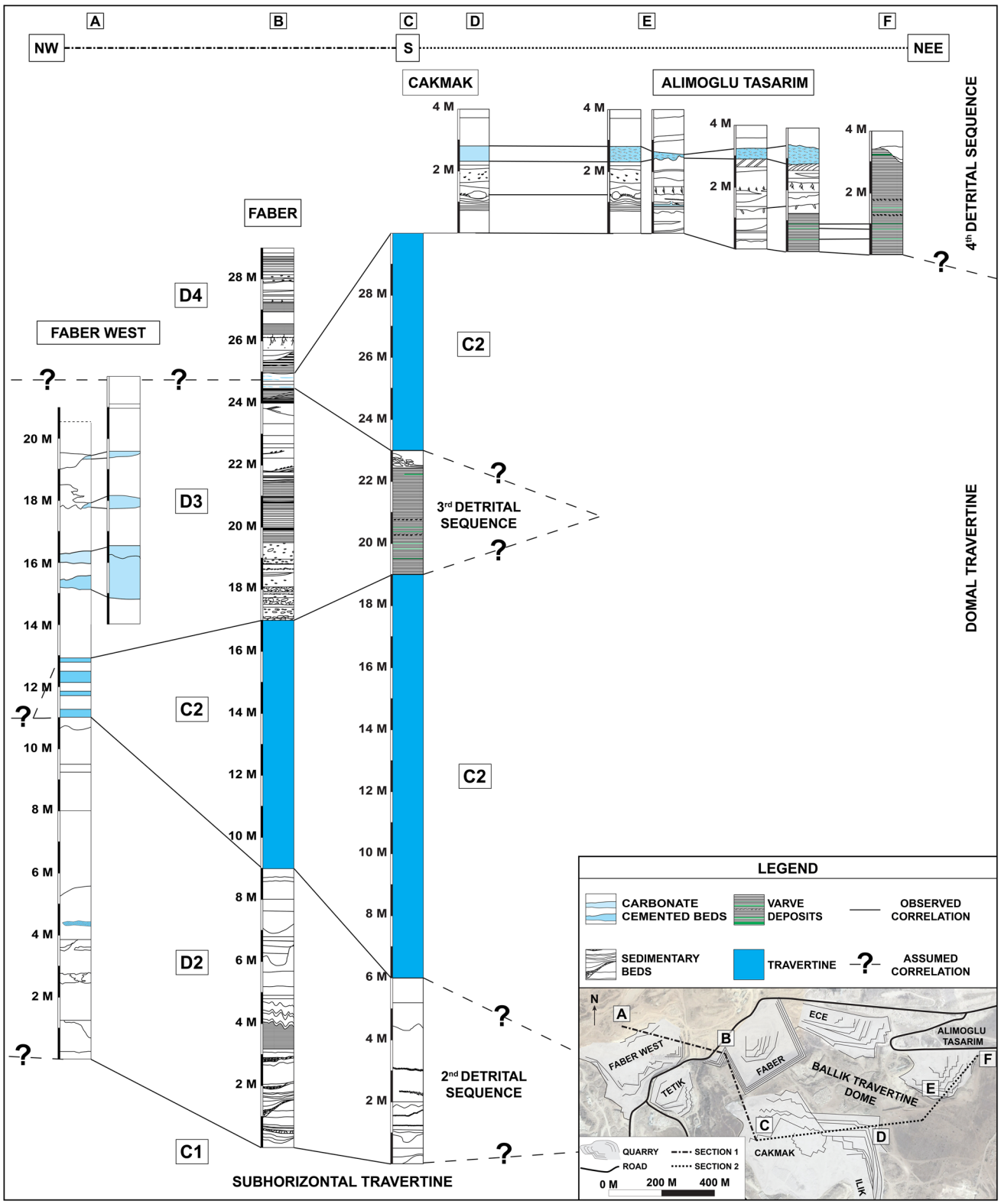

Fig. 5 Simplified log correlation of the detrital sequences in the Ballık area. The first detrital sequence (D1) is not presented in this figure due to its local development

laminated marls and domal travertine lithologies is characterised by interfingering geometries (Fig. 6a), which have been accentuated by differential compaction. At a greater distance from the domal structure, two sub-successions were observed, both consisting of conglomeratic channels and tabular sandstones, which are covered by laminated marls. Each succession starts with the deposition of erosive conglomerates, intertwined with tabular sandstones, which are gradually replaced by laminated marls (Fig. 5). Between both successions, an erosive contact is observed, followed by the overlying sequence starting with erosive conglomerates. In addition, root traces are present in laminated marls underneath this contact (Fig. 6b).

The fourth and youngest detrital sequence is only observed on top of the quarries of Alimoğlu-Tasarim, Çakmak, and Metamar abandoned (Fig. 3). The total thickness of this sequence, which consists of two different sub-successions, varies between 4 and 10 m. The lower sub-succession consists of laminated marls, in which root traces and gastropods are abundant. An erosive contact separates the lower from the upper sub-succession, which is dominantly made of grain-supported conglomeratic beds, tabular sandstones, and gastropod-rich carbonates. In addition, ball-and-pillow structures were observed throughout this sequence, within all mentioned quarries (Fig. 6c).

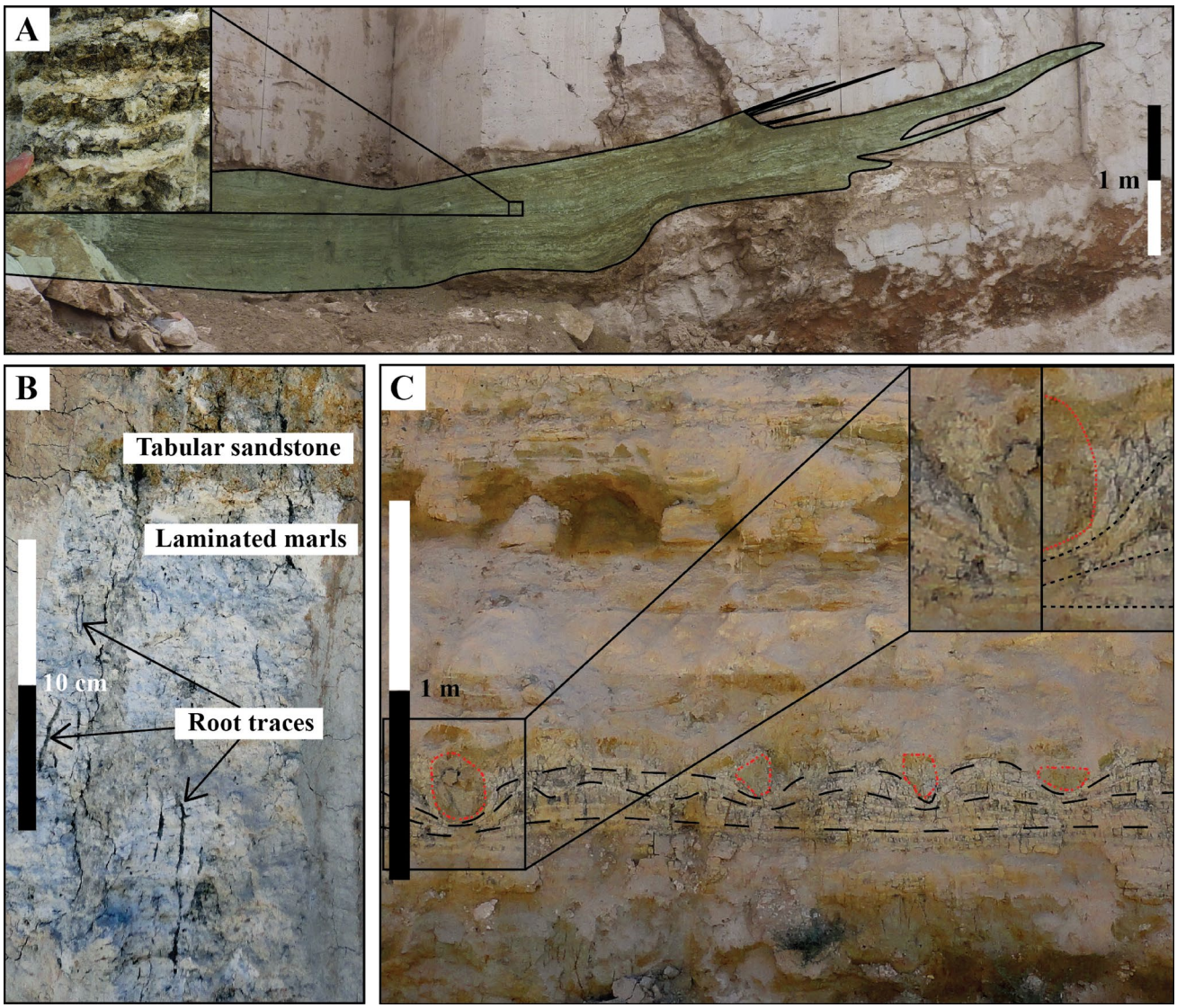

Fig. 6 Laminated marl deposits. **a** Wedge-shaped laminated marls interfingering with travertine in the Çakmak quarry with inset of a detailed zoom on varve-like features. **b** Root traces in laminated marls at the erosive contact with the overlying tabular sandstones. **c** Ball-and-pillow structures on the contact between laminated marls and tabular sandstones, highlighted in red

Detrital lithologies

In total, five different detrital lithologies could be differentiated, i.e., laminated marls, polygenetic conglomerates, massive marls, tabular sandstones, and coquina accumulations. All sequences, except for the first detrital polygenetic conglomerate (D1), contain several of these lithologies.

Laminated marls

Up to 12-m-thick and laterally extensive outcrops (dimension up to > 200 m by 500 m) of laminated marls are exposed in the analogue system. The latter represent a minimum estimated volumetric share of 65% of all detrital lithologies, based on the exposed detrital sediments. These marls are characterised by fine-grained particles, deposited as alternating brown or green laminae with a thickness between 0.5 and 4 cm. In general, the carbonate content, and thus the degree of cementation, of this lithology increases with the proximity to travertine lithologies, where intertwining geometries can be observed (Fig. 6a). Throughout the laminated marls, root traces are abundant proximal to travertine lithologies, whilst they are scarce at larger distances from these lithologies. Root traces were also often observed in the proximity of erosive surfaces, which are succeeded by other lithologies such as tabular sandstones (Fig. 6b). Noteworthy is that bioturbations were absent throughout these laminated marls.

Microscopically, laminated marls consist of an alternation of clay-bearing packstone-to-wackestone laminae. Packstone laminae have a white colour and dominantly consist of a mixture of sub-angular quartz and calcite grains, ranging from 20 to 100 µm in size (Fig. 7a). In the dark green-coloured wackestone laminae, micrite, peloids and clay minerals are more abundant. Laminated marls, consisting of pluri-centimetric alternations of pack- to wackestone laminae, are observed throughout the Ballık area. In addition, algal structures were frequently observed, with either branching or horizontally laminated geometries (Fig. 7b). Intact ostracods are present throughout these lithologies, but preferentially occur in the wackestone laminae (Fig. 7c). Beside these bioclasts and detritals, also some diagenetic phases could be identified such as zoned calcite phases under cathodoluminescence and authigenic clays. Cathodoluminescence microscopy revealed the presence of calcite rims covering sub-angular detrital grains of quartz and calcite (Fig. 7d). These rims are made of alternating bright and non-luminescent calcite phases. Up to three (sometimes incomplete) successions were observed (Fig. 7d). These rims are circumgranular, or exhibit dissolution features, creating irregular shapes, recognisable by the abrupt interruption of discontinuous rims. These phases often have a preferential growth direction, which varies for different adjacent grains. Calcite rims were observed more abundantly and are more pronounced in laminated marls proximal to the travertine dome, where intertwining geometries between both lithologies are observed and where the degree of cementation is higher (Fig. 6a). In general, a final cement phase, welding together several individual detrital grains was often observed in the thin sections. SEM observations confirmed the presence of this final cement phase, causing individual detrital grains to form aggregates (Fig. 7e).

In addition to the abundance of calcite, quartz and clay minerals, bulk XRD measurements also highlighted the presence of dolomite within these laminated marl lithologies. Based on the broad appearance of the 104-diffraction peak, the dolomite phases appear to consist of poorly ordered dolomite crystals (Nash et al. 2013 and Rodriguez-Blanco et al. 2015). However, dolomite grains are rarely observed by cathodoluminesence in thin sections, suggesting that the fraction of dolomite is rather fine-grained. The latter is in line with SEM observations in which dominantly clusters of small rhombohedrons (3 µm) were observed (Fig. 7f).

Diffraction patterns revealed the presence of six different clay minerals. In the 7 Å region, chlorite, kaolinite, and serpentine could be differentiated based on their respective basal diffraction at 7.07 Å, 7.17 Å, and 7.31 Å, respectively (Bayliss et al. 1986). The ethylene–glycol saturated slides revealed the presence of smectite and interstratified R0 illite–smectite based on their swelling behaviour. All of these clay minerals were already identified in bulk mineralogical measurements; however, oriented clay slides also revealed the presence of palygorskite, displaying a peak at 10.5 Å. Palygorskite bridges in between detrital grains and/or detrital grains encased by palygorskite fibres confirm the authigenic origin of these clays (Fig. 7e). In addition, quartz grains are characterised by dissolution features, covered by palygorskite fibres.

Polygenetic conglomerates

Polygenetic conglomerates possess erosive bases, above which in general a fining upward succession develops with pebbles displaying imbrication structures (Fig. 4c). The lateral width of these conglomeratic bodies varies from 1 to 15 m and the vertically amalgamated channel-like structures can reach thicknesses of up to 6 m (Fig. 4a, b). Several adjacent and fining upward conglomeratic beds regularly occur, likely reflecting simultaneous deposition within a fluvial system (Fig. 8a). An additional characteristic of these conglomerates is the varying orientation of the imbrication structures in amalgamating channels, indicating different flow directions present in the system, which was generally dominated by a southerly flow direction (Fig. 4c). Clasts vary in size between 0.5 and 30 cm. Smaller clasts are generally well rounded, while larger clasts often have an angular shape. In general, large

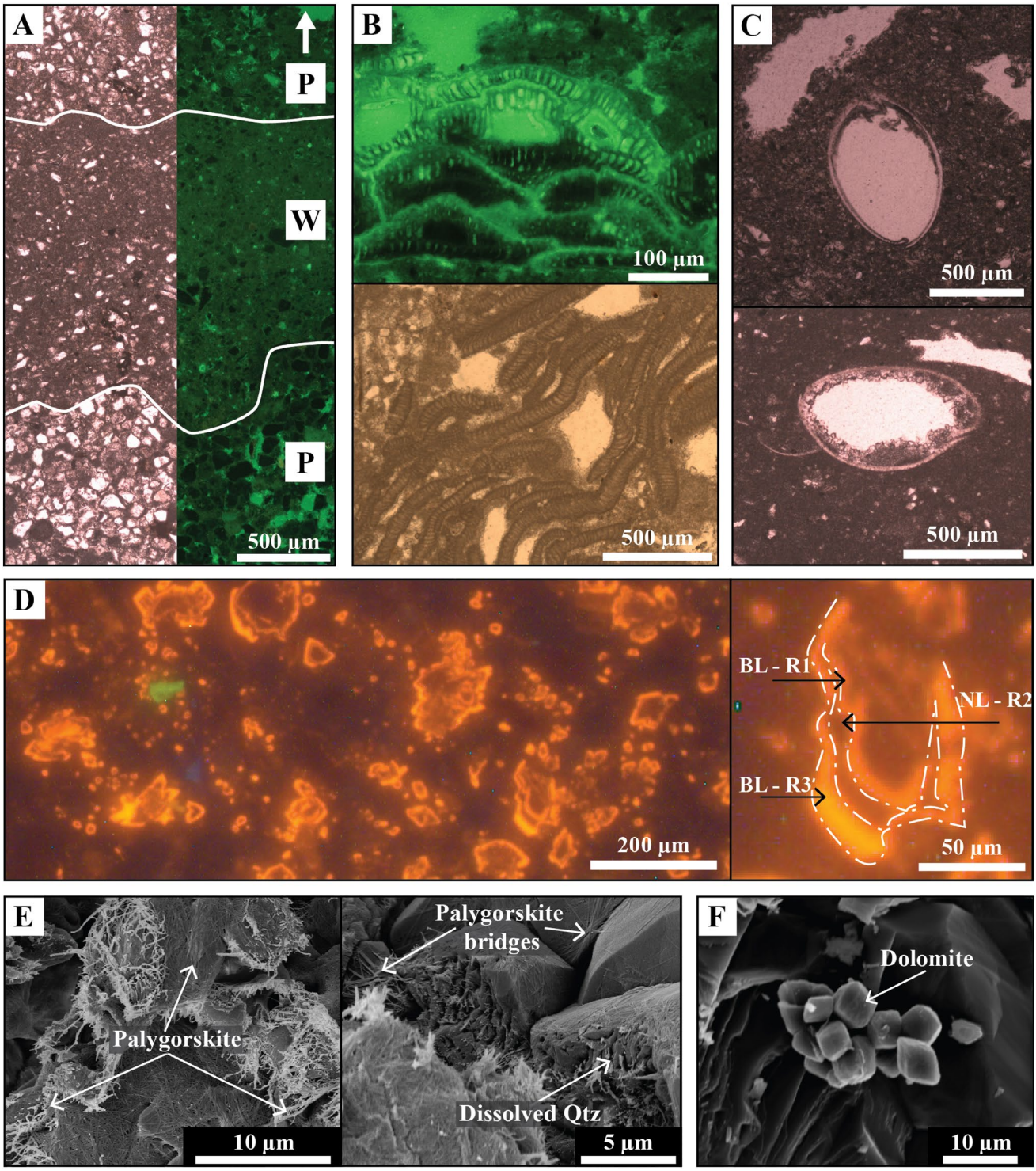

Fig. 7 Petrography of laminated marl deposits. **a** Microscopy image of alternating packstone (P) and wackestone (W) laminae (left—transmitted light and right—fluorescence microscopy). **b** Algal structures observed in lacustrine sediments, both with build-up geometries (top) and elongated geometries (bottom). **c** Intact ostracod in wackestone laminae. **d** Detailed image of zoned calcite rims (R1, R2, and R3), consisting of alternating bright luminescent (BL) and non-luminescent (NL) cements, with the preferential growth direction highlighted by a white arrow. **e** SEM petrography of lacustrine sediments, highlighting a dense palygorskite network (left). Quartz grains were characterised by dissolution features and with palygorskite bridges (right). **f** Cluster of dolomite rhombohedrons with a dimension of about 3 µm, present on the surface of detrital grains

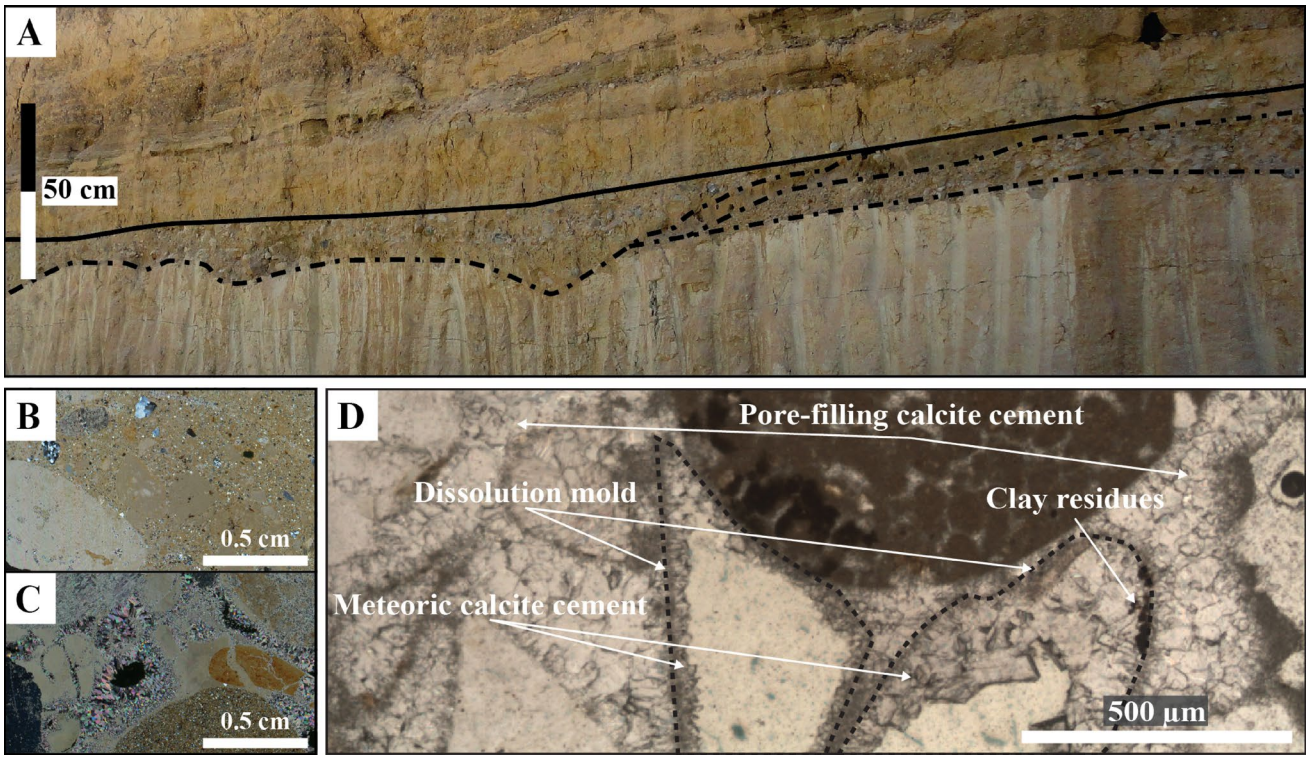

Fig. 8 Polygenetic conglomerates. **a** Outcrop showing different conglomeratic channels simultaneously deposited with erosive surfaces highlighted in black. **b** Thin section of mud-supported conglomerate lithotype, with clasts embedded in a calcareous matrix. **c** Thin section of cemented and grain-supported conglomerates. **d** Detailed image of dissolution molds in cemented conglomerates, with the presence of clay residues

boulders are made of laminated travertine similar to the sub-horizontal travertine described by Claes et al. (2015). This is in contrast to finer clasts, which are made of a mixture of quartzite, limestone, dolomite, marble, gneiss, and serpentinite, in correspondence with the geology of the broader provenance area as described by Sözbilir (2002) and Khatib et al. (2014). The size and angularity of these clasts likely reflect the distance from the source area, where large and angular boulders of sub-horizontal travertine are eroded locally, as the fragile nature of the travertines would not survive such transport over large distances.

Two different types of conglomerates were recognised in the Ballık area, characterised by a different degree of cementation. At a greater distance from the Ballık travertine dome, the conglomeratic matrix consists of a microporous micrite leading to mud-supported and poorly cemented conglomeratic beds (Fig. 8b). Proximal to the travertine dome, conglomerates are welded together by a crystalline calcite cement, yielding well-cemented and grain-supported conglomerates (Fig. 8c). Within the latter, mouldic pores are observed which are filled with meteoric drusy calcite cements (Fig. 8d). In addition, clay residues and iron (hydr) oxides border the dissolution moulds.

Massive marls

Brown massive marls are characterised by the lack of any internal structure; this in contrast to laminated marls. Additionally, floating pebbles were often observed in a mud-supported matrix. These pebbles were dominantly composed of travertine, with sizes ranging from 0.2 to 5 cm. As illustrated in Fig. 9a, massive marls were often observed in the vicinity of polygenetic conglomerates and always have a rather limited thickness (up to 1 m). In the proximity of these conglomeratic beds, reed-like structures were present in the massive marls. The top of this lithology is often characterised by an erosive surface marked by manganese oxide-stained root traces, implying a temporary subaerial depositional environment. In addition, it was observed that the degree of calcite cementation increased with closer proximity to the conglomeratic beds. The latter is an indication that these conglomerates acted as a preferential flow path for the fluids that cemented both the conglomerates and adjacent lithologies.

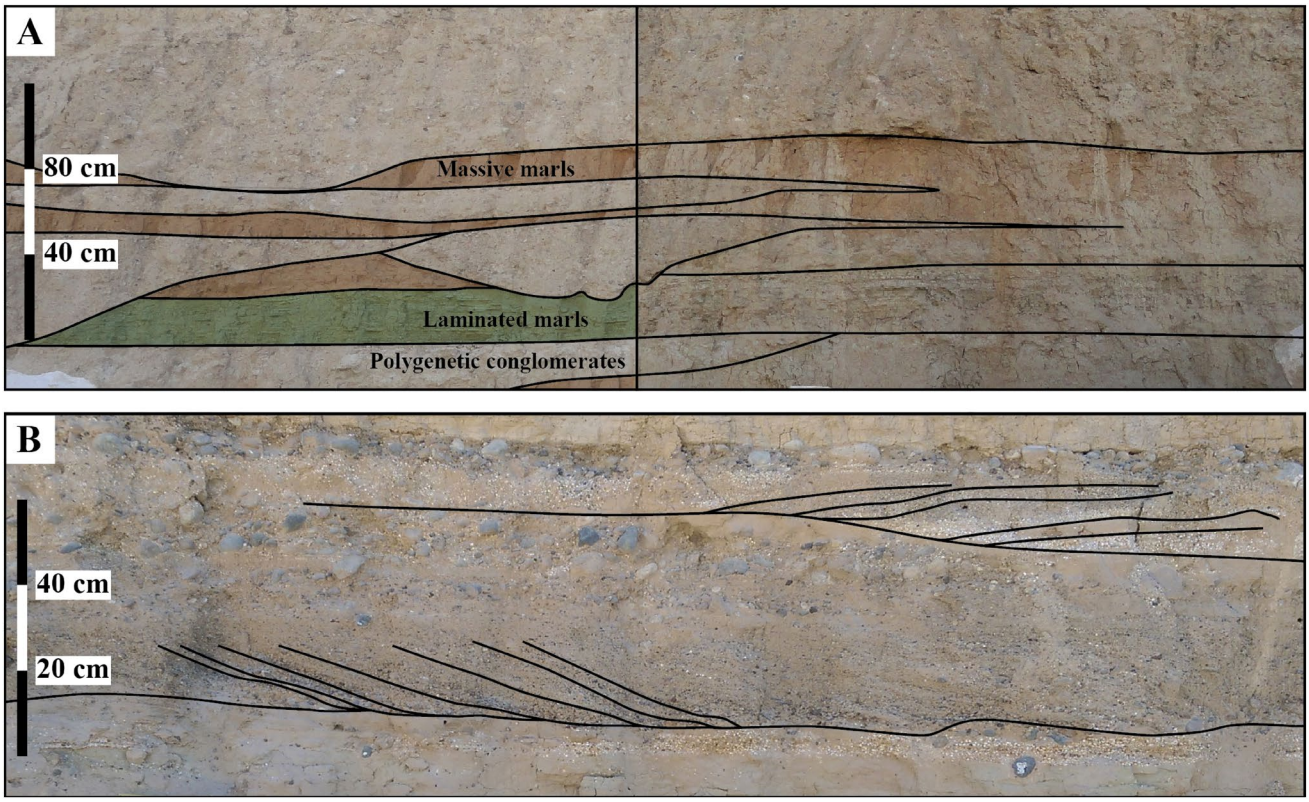

Fig. 9 Fluvial lithologies. **a** Outcrop with different fluvial lithologies, occurring next to each other, interpreted as a floodplain. **b** Example of tabular sandstones with cross bedding and crushed gastropod shells, occurring in the vicinity of conglomeratic beds

Tabular sandstones

Tabular sandstones are closely associated with polygenetic conglomerates and massive marls, indicating a similar depositional environment (Fig. 9a). The thickness of these tabular sandstones is generally limited to 20 cm, while they are laterally continuous for up to 500 m. They consist of medium-to-coarse sands and often display unidirectional cross bedding (Fig. 9b). These tabular sandstones are generally characterised by a planar base, in contrast to the polygenetic conglomerates that are characterised by incision channels. In general, broken shell fragments of gastropods were present throughout this lithology, which are more abundant at their base. Some of the tabular sandstones were characterised by a general vertical fining upwards trend. Furthermore, ball-and-pillow structures are present in tabular sandstones on top of the laminated marls (Fig. 6c). Due to the unconsolidated nature of these sandstones, sampling was virtually impossible. Therefore, no additional petrographic observations were performed in this study.

Coquina accumulations

Coquina accumulations were observed in the proximity of laminated marls and at the base of some of the tabular sandstones. Their dimensions are limited to 50 cm in thickness and 20 m in horizontal extension. Two different types of gastropod-bearing beds were observed, being either of a carbonate-rich and well cemented or of a poorly cemented lithotype. The first type (Type I) occurs in proximity of the travertine dome, and is dominantly made of moulds of (originally intact) gastropod shells, concentrated into certain horizontal layers, and embedded in a micrite matrix, in which coarse-to-very coarse detrital grains were observed (Fig. 10a, b). Dissolution of these gastropod shells after deposition resulted in mouldic porosity. The second type (Type II) is associated with the presence of tabular sandstones and is dominantly made of both intact and crushed gastropod shells, which can be up to 7 mm in size (Fig. 10c). In general, the second type consists of a sandy matrix rich in pebbles, often displaying cross-laminations. In contrast to the carbonate-rich and well-cemented type, the matrix

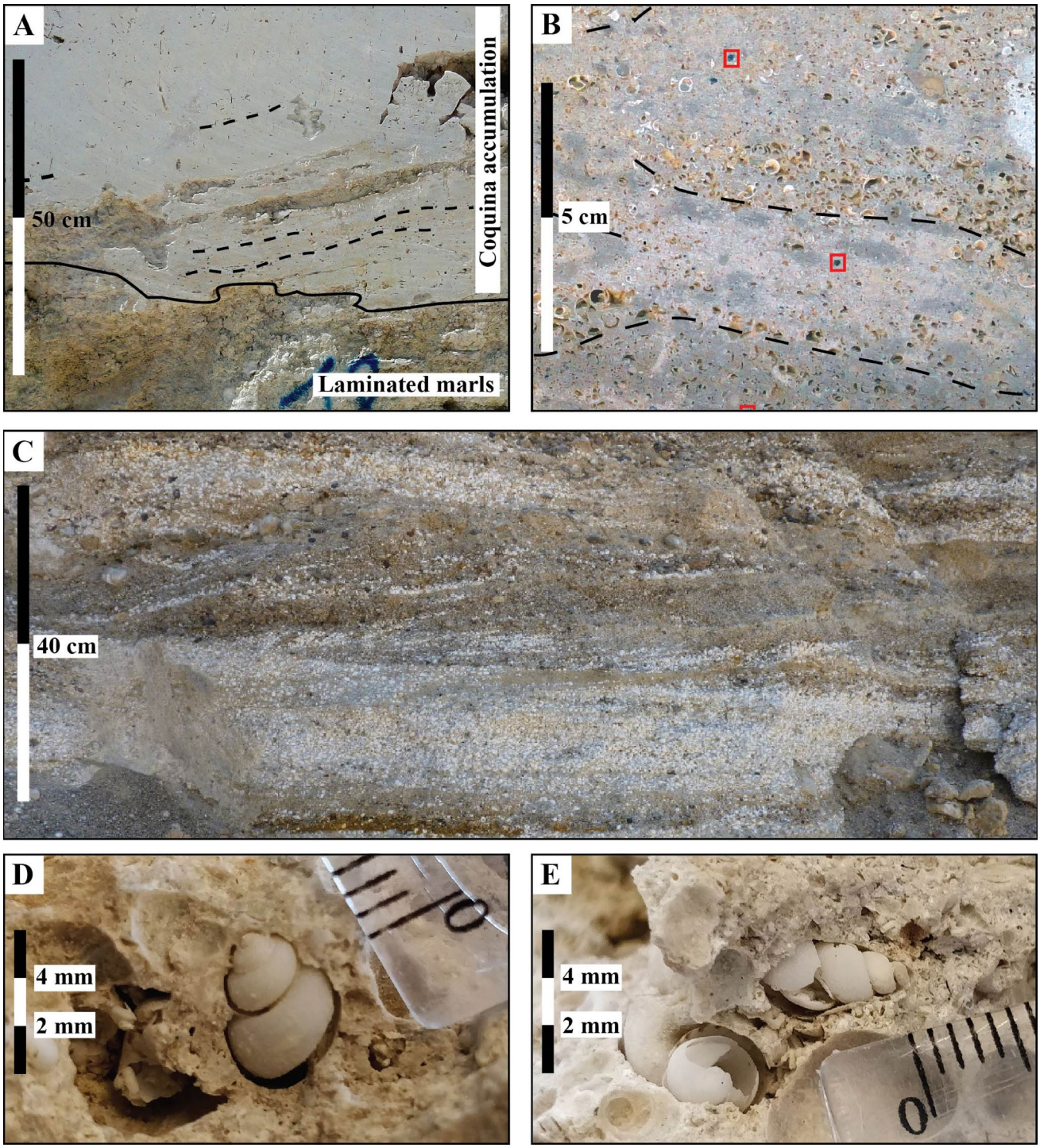

Fig. 10 Coquina accumulation. **a** Subhorizontal aligned coquina accumulations (Type I), bordering lacustrine and travertine deposits. **b** Subhorizontally aligned coquina accumulations with detrital fragments (red). **c** Thick coquina accumulations (type II), displaying cross bedding surrounded by fluvial lithologies. **D**, **e** Macroscopic image of gastropods from the Hydrobiidae family, observed in the Ballık area

of these beds was unconsolidated, making it impossible to properly sample this lithology for petrographical analysis.

The gastropod shells were identified to belong to the Hydrobiidae family, which is known to be a large family of freshwater gastropods, characterised by a high diversity due to the occupation of fragile and restricted ecosystems (Delicado et al. 2013). Due to the poor conservation, it

was impossible to identify the specific genus or species of these gastropods (Fig. 10d, e).

Petrophysical properties

Petrophysical properties for two lithologies, i.e., polygenetic conglomerates and coquina beds, were assessed during this study. 2D porosity in laminated marls was estimated through image analysis.

In general, polygenetic conglomerates are characterised by a scattered, but positive correlation between porosity and horizontal permeability (Fig. 11). Polygenetic conglomerates are characterised by a wide range of porosities (5.5–15%) and permeabilities (0.02–3000 mD) and depending on the matrix a different trend can be observed. Crystalline carbonate cements in polygenetic conglomerates significantly reduce their pore volume, while their permeability can still be relatively high. Carbonate muds in the mud-supported conglomerates tend to lead to low permeability values, while the matrix itself contains a significant amount of microporosity. Therefore, calcite-cemented polygenetic conglomerates are characterised by relatively low porosities and high permeability values, while mud-supported polygenetic conglomerates are characterised by elevated porosities and reduced permeabilities. Porosity values for coquina accumulations are elevated (8.5–4%), while yielding low permeabilities (0.04–0.26 mD). 2D-porosities for laminated marl lithologies, based on 5 samples, range between 4. 1 and 19. 3% (not plotted in Fig. 11).

Discussion

The detrital lithologies can be linked to a specific facies based on different characteristics reflecting different depositional settings. The lower part of the succession is dominated by a lacustrine setting, in which wedge-shaped laminated marls were deposited on top of sub-horizontal travertines. The latter were interpreted by Claes et al. (2015) to be deposited in depressions in a palustrine-to-lacustrine environment. Along the shorelines of these lakes gastropods are accumulated, corresponding to the coquina beds of the shoreline facies. In addition, fluvial facies are also represented in the detrital lithologies, corresponding to the channel-shaped conglomerates, massive marls, tabular sandstones, and isolated coquina beds.

Quaternary sediments in the Ballık area either consist of detrital deposits or continental carbonates. Both types are either observed to dominate the sedimentary record entirely or can occur simultaneously next to one another (Fig. 3). Both climatological changes and tectonic activity are plausible mechanisms capable to explain changes in the depositional environment; however, this study focussed specifically on the sedimentary aspects of the different detrital

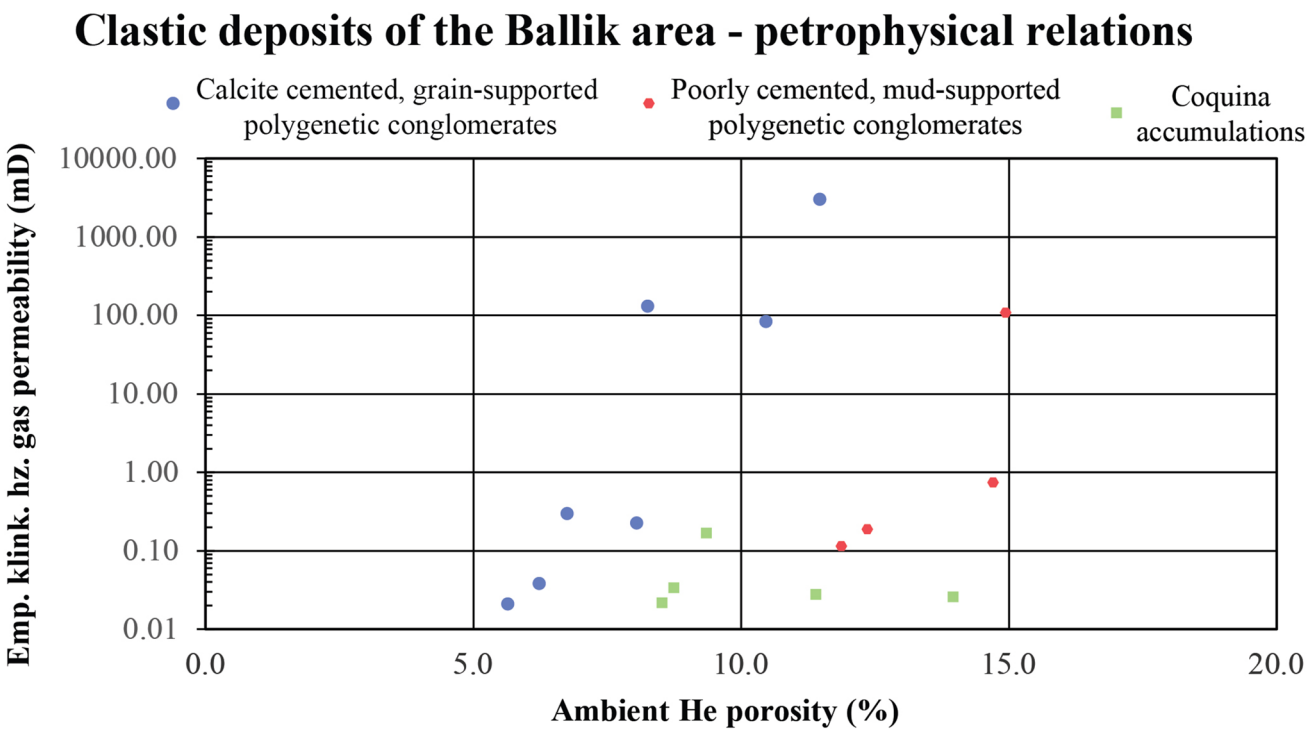

Fig. 11 Measured He-porosity (%) and empirical Klinkenberg corrected horizontal gas permeability (mD) on a semi-logarithmic plot. The data show a scattered, but positive correlation

lithotypes in the Ballık area. Therefore, no detailed analyses of climatological proxies or of specific relationships between tectonic activity and sedimentation were carried out in the frame of this study. Based strictly on our observations, and to explain the changes in the depositional environment, only hypothetical assumptions are thus presented in this section. As described by numerous authors, i.e., Gawthorpe et al. (1994), Gawthorpe and Leeder (2000) Serck and Braathen (2019), tectonic activity might create accommodation space by the creations of topographic lows due the activation of normal faults. However, observations made throughout the different recognised facies tend to support climatological changes in favour of tectonism (Table 1). Even though post-depositional ball-and-pillow structures were observed in certain quarries of the Ballık area, they do not necessarily imply strong tectonic events capable of creating significant accommodation space (Fig. 6c). In addition, no synsedimentary deformational structures were observed during this study. Therefore, we conclude that most tectonic activity within the study area took place after sediment deposition, which is in line with the detailed tectonic study from Van Noten et al. (2013). However, activation of normal faults in the broader region surrounding the study area might have led to the formation of fault scarps. The latter are associated with the formation of alluvial fans, which might explain the influx of conglomerates in the study area (Carncicelli et al. 2015; Walk et al. 2019). Although no direct evidence of tectonic interference was observed in the well-exposed 3 km by 2 km study area, an external tectonic control cannot be excluded, neither confirmed, considering the overall geodynamic context.

Lacustrine facies

The lacustrine facies, corresponding to the laminated marls, was observed in all quarries. With an estimated volumetric share of 65% of all detrital lithologies, it is thus the most abundant detrital facies of the Ballık area. This facies reflects paleo-lows, often occurring in close proximity of the Ballık travertine structure. Both the presence of laminae, the thickness (up to 12 m) and the aerial extension of these laminated marls, are indicators for an extensive and continuous depositional setting. The latter is also supported by the widespread interfingering, under- and overlying sub-horizontal travertine lithologies (Fig. 6a). Furthermore, laminae proximal to the travertine dome are characterised by an increasing degree of cementation with increasing proximity to the travertines, implying that laminated marls are time-equivalents of the adjacent travertines. The local and temporary absence of these travertine lithologies, during the deposition of the lacustrine detrital sediments, reflect (1) an increased influx of detrital components such as quartz and clays and (2) a dilution of the travertine precipitating fluids (either due to lowered spring activity or due to mixing with meteoric waters). A possible explanation is a long-term increase in the amount of rainfall, possibly reflecting a climatological shift towards a continually rainfall-dominated time period. Although tectonism might also lead to the creation of accommodation space, and thus lead to topographic depressions where lakes could form, no evidence for strong synsedimentary tectonics was observed, as mentioned above.

Varves

Next to the fragile algal structures and intact ostracods, preserved laminae are an indicator for a calm, shallow and restricted depositional environment. The rhythmically alternating laminae have similar visual characteristics as varves, however, the latter generally have millimetres-scaled thicknesses (Boehrer and Schultze 2008; Zolitschka et al. 2015). This is in contrast to laminae observed in the Ballık area, which can have thicknesses of up to several centimetres. These rather thick laminae are an indicator for an elevated sedimentation rate, potentially linked to the associated precipitation of CaCO3 from supersaturated waters within these lakes (Ma et al. 2017). The latter indicate that travertine sources were still active in the area, but increased rainfall diluted runoff waters in these lakes, whilst increasing the

Table 1 Arguments in favour of climate-driven changes in the depositional environment

Deposit type	Characteristics	Interpretation
Lacustrine	–Widespread and thick deposits –Continuous laminae –No asymmetry within lacustrine basins	–No significant tectonic disruption for a longer time period –No significant synsedimentary tectonism, otherwise these would be disrupted –Absence of synsedimentary growth faults
Fluvial	–Gradual transition between different lithologies –Absence of mudflows and/or landslide deposits –Absence of boulders –Wadi-system	–No abrupt transitions, which would be expected by tectonism –Would be expected in case or tectonic activation of nearby fault systems –No significant differences in terrain –Fault-controlled systems would lead to fan-type conglomerates
Travertine	–Widespread and continuous deposits –Feeder faults are rarely observed –Gradual transition from sub-horizontal travertines (palustrine) to lacustrine system	–No significant tectonic disruption for a longer time period –Synsedimentary faults are rather local features –Gradual on lap of lacustrine sediments would not occur if accommodation space would rapidly change due to tectonism

input of detritals. Furthermore, the absence of bioturbations within laminated marls indicates that at least the deeper parts of these lakes were characterised by suboxic-to-anoxic conditions, a setting which is further addressed below when discussing the formation conditions of zoned calcite rims.

The repetitive laminae are tentatively interpreted to reflect cyclic variation throughout the year. Two different conditions are required to explain the rhythmic alternation of packstone and wackestone laminae (Fig. 7a). There were likely periods with a high influx of meteoric water (wet seasons), while during other periods, lake water was dominated by runoff waters from the travertine system, corresponding to fracture- and fault-derived hydrothermal water (dry seasons). Packstone laminae require a high-energy hydrodynamic depositional environment, in which detrital quartz and calcite grains are actively supplied to the lake system. These periods are likely to correspond to periods of increased rainfall and detrital runoff, while simultaneously calcite saturated waters were still being provided by the adjacent travertine seep system. During dry seasons, the freshwater supply will diminish, reducing input of both fresh water and coarse-grained detrital components in the lacustrine system. The latter, in combination with evaporation, will give rise to a more stagnant or shrinking water body of the lake. These calm conditions allow clay and fine-grained calcite fractions to settle down, forming wackestone laminae (Ma et al. 2017; Valero-Garcés et al. 2014). These systematic lake-level fluctuations will thus lead to the formation of (1) varve-like alternations of wackestones and packstones and (2) zoned calcite rims, which are addressed below (Fig. 12).

Eogenetic processes

The calcite rims, encasing detrital grains, are characterised by an alternation of bright and non-luminescent calcite zones and often display a preferential growth direction. The latter is not always oriented in the same direction for all observed calcite zonations (Fig. 7d). The presence of a final calcite phase, welding together individual detrital grains into aggregates, is an indicator for in-situ aggregation of these

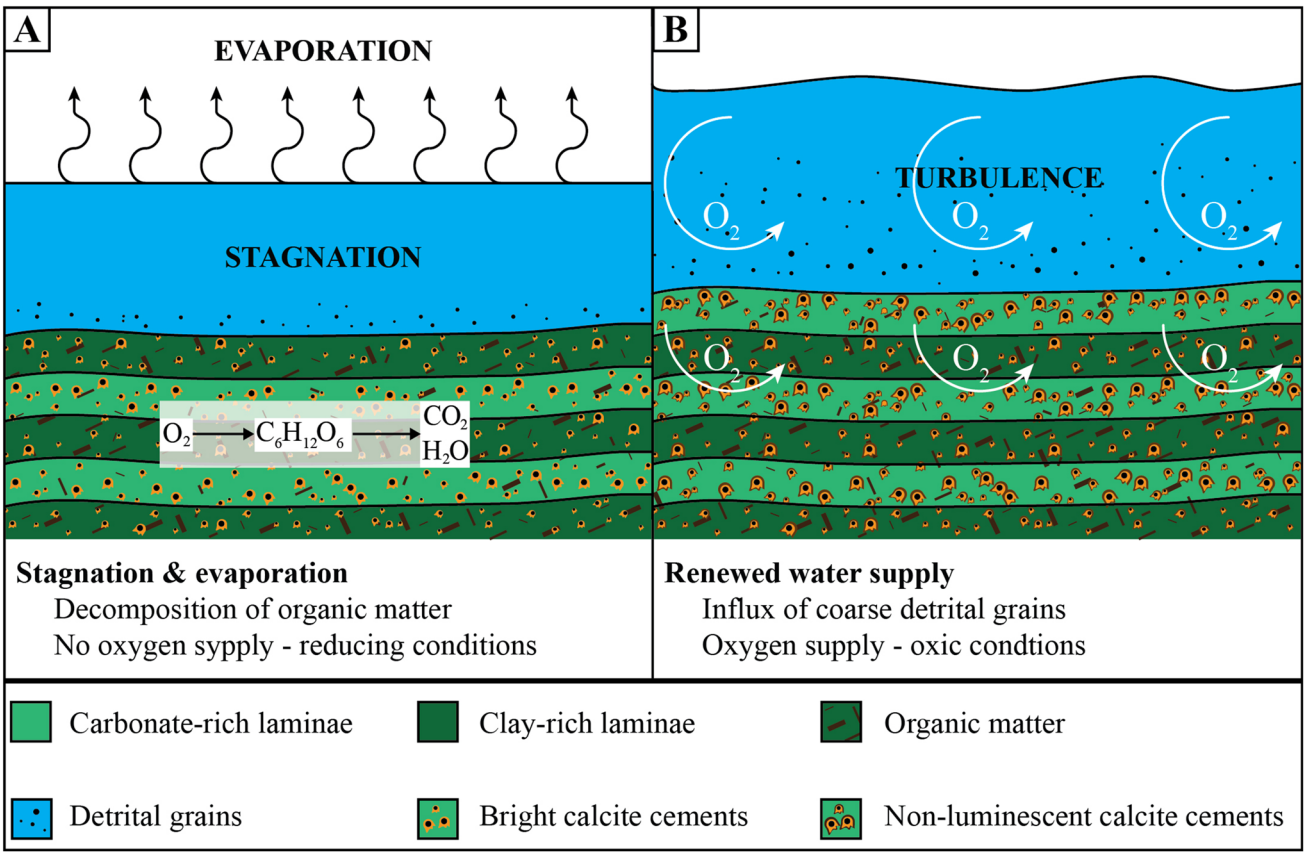

Fig. 12 Illustration of the conditions of formation of zoned calcite rims. **a** Lake sediments with stagnant lake waters, decreasing oxygen supply in lacustrine sediments. Stagnation and concomitant decomposition of organic matter results in suboxic conditions, favouring the formation of bright calcite cements (dry seasons). **b** Periods of renewed water supply leading to turbulence, causing oxygen levels in the lacustrine sediments to increase. The latter leads to more oxic conditions, in which non-luminescent calcite cements formed (wet season)

calcite rims. Otherwise, aggregates would have disintegrated due to erosion during transport; however, limited reorientation of the grains could have occurred. Zoned calcite grains are observed throughout all lacustrine sediments in the study area, but preferentially occur near the margins of former lake bodies, proximal to the travertine dome. Since these zonations are not isolated phenomena, they require a mechanism capable of generating favourable conditions of formation over a wide area, but preferentially in close proximity to the travertine lithologies (Fig. 6a).

A possible argument for this spatial relationship is the saturation state of the pore water near the lake margins. Due to the influx of Ca-rich runoff waters from the geothermal springs, where travertine formation actively took place, calcite saturation would be high (Fig. 13). These saturated pore waters lead to suitable conditions for the formation of these zoned calcite rims. In addition, these zonations reflect changing crystallisation conditions; however, due to the scale of these small calcite rims, no geochemical constraining data are available. A likely hypothesis explaining their formation, reflecting changing geochemical conditions, relates to variations in lake water geochemistry. The proposed mechanism links the bright calcite cements to suboxic conditions, as described by Boggs and Krinsley (2006), precipitating in stagnant lake bodies, with a limited influx of fresh water (Fig. 12a). The latter conditions will decrease oxygen availability in lacustrine sediments and allow fine-grained sediments to settle, causing wackestone laminae to form (Ma et al. 2017; Valero-Garcés et al. 2014) (Fig. 7a). Oxygen consuming reactions, associated with decomposing organic material, will further enhance suboxic conditions within the sediments. The alternation between wet and dry seasons likely caused lake levels to fluctuate during the deposition of these sediments. At the start of the wet season, a renewed influx of fresh water in the lake system will supply oxygenated water and increase turbulence, resulting in conditions favourable for the formation of non-luminescent calcite rims (Fig. 12b). In addition, this turbulence will lead

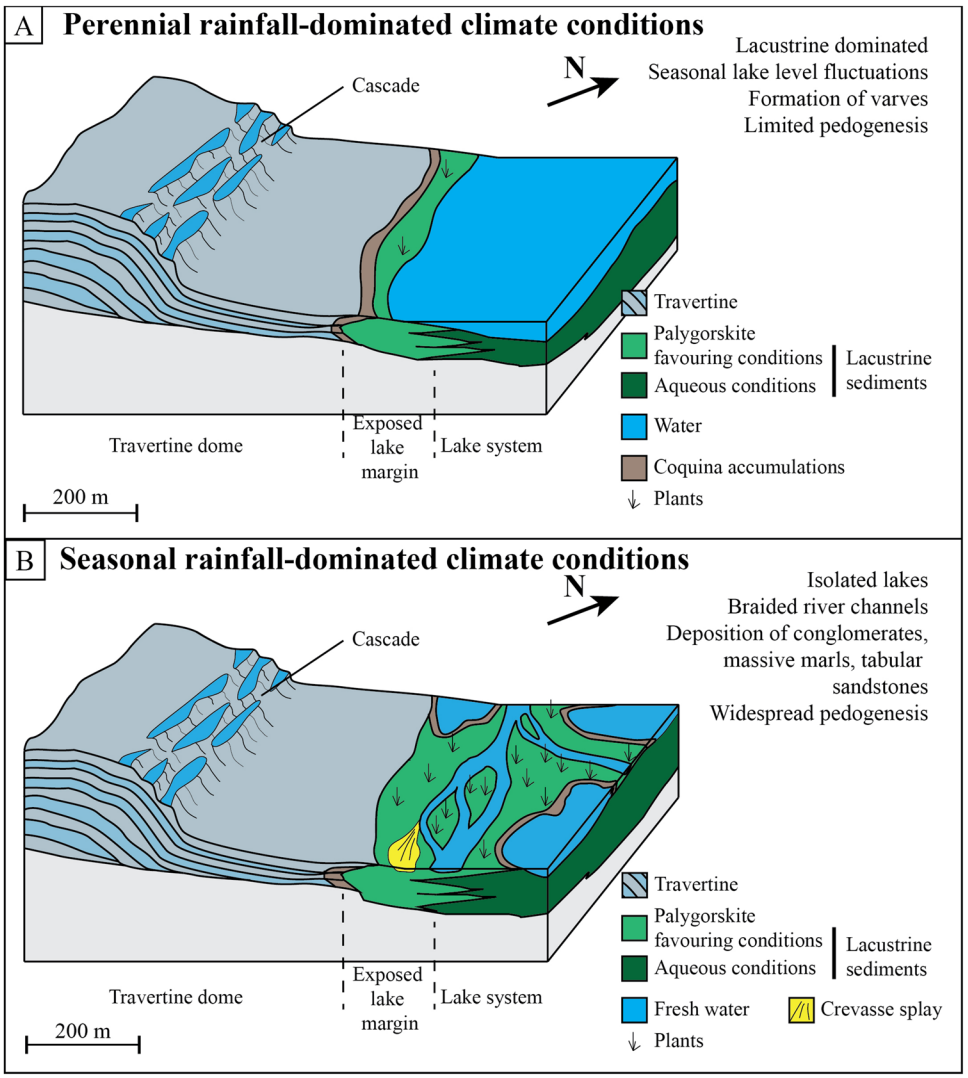

Fig. 13 Conceptual depositional model for the lacustrine, fluvial, and shorelines facies. **a** Depositional model (1 km by 600 m) for the detrital sedimentary system during perennial rainfall-dominated climate conditions, leading to a lacustrine-dominated system with limited pedogenesis. Seasonal cyclicity causes lake-level fluctuations, leading to the deposition of varves-like couplets. Coquina accumulations (type I) are deposited along the shoreline. **b** Depositional model for the lacustrine system for seasonal rainfall-dominated conditions (semi-arid), significantly lowering lake levels leading to a fluvial-dominated system. Deposited lake sediments will be subaerially exposed, giving rise to widespread pedogenesis favouring the formation of palygorskite and dolomite. Isolated pools exist between different river channels, associated with local coquina accumulations (Type II). Heavy rainfall might give rise to local deposits of tabular sandstones, corresponding to crevasse splays

to the deposition of packstone laminae, while fine particles will remain in suspension. During the dry season, the lake body would become stagnant, while carbonate saturation would increase. Repetition of these cycles, throughout successive years are thus a plausible explanation for the formation of these zoned calcite rims in laminated marls. In addition, a varying degree of calcite saturation explains the dissolution features that give rise to the observed irregularly shaped rims.

The presence of palygorskite and poorly ordered dolomite are important observations to constrain eogenetic processes that occurred after deposition of these lacustrine sediments. Rodas et al. (1994) and Xie et al. (2013) considered palygorskite as a tracer for arid conditions. Botha and Hughes (1992) suggested that palygorskite forms in subaerially exposed lacustrine sediments during semi-arid pedogenesis. Sedimentary features supporting these processes, such as glaebules, cracks, and calcrete formation, were not observed, potentially due to the rather short period during which pedogenesis took place. Associated with authigenic palygorskite is the precipitation of authigenic and poorly ordered dolomite, directly out of soil solutions (Botha and Hughes 1992). Calcite precipitation (the so-called calcite rims) lead to pore water with an increased magnesium-to-calcium ratio. The latter possibly facilitated dolomite formation in the exposed lacustrine sediments. The wide 104-diffraction peak reflects the extremely small size of the dolomitic grains, which are interpreted to reflect a poorly ordered crystallographic nature (Nash et al. 2013). Observations supporting subaerial exposure were observed in all quarries, ranging from manganese oxide-rich root traces (indicating that plants grew in these lacustrine sediments) to erosive surfaces (Fig. 6b). Pedogenesis is thus an indicator for subaerial exposure of the lacustrine sediments, interrupting the deposition of lacustrine sediments. In addition, the top of these lacustrine sediment packages is characterised by erosive surfaces, possibly indicating temporary shifts towards a more arid climate with short periods of heavy rainfall. The latter is also supported by the presence of river channel deposits, reflecting the transition from a lake-dominated depositional system towards an erosive and fluvial-dominated system. It is these longer term, arid conditions that are required for the pedogenic formation of authigenic palygorskite and poorly ordered dolomite (Botha and Hughes 1992; Rodat et al. 1994).

Depositional model

The depositional model of the lacustrine facies thus has to incorporate the widespread deposition of rhythmic laminated lacustrine sediments, authigenic palygorskite, and dolomite (with corresponding evaporative conditions and temporary pedogenic processes) (Fig. 13). The widespread dominance of lacustrine systems is likely to correspond to a long-term period dominated by a wet climate, associated with the predominance of the input of detrital sediments (Fig. 13a) (Gierlowski-Kordesch et al. 2013; Renaut et al. 2012) and/or favourable tectonics creating the accommodation space for the development of a shallow lake. Since no indications of synsedimentary tectonic activity were observed, in line with the study of Van Noten et al. (2013) who concluded that most tectonic activity postdates the formation of the Ballık travertine dome, the transition towards a wet climate is the most plausible mechanism capable to explain the widespread lacustrine sediments and the influx of detritals. Furthermore, variations in the hydrological regime are required to explain the rhythmic alternation of packstone and wackestone laminae (Fig. 7a). These systematic lake-level fluctuations will thus lead to the formation of (1) varve-like alternations of wackestones and packstones and (2) zoned calcite rims (Fig. 12). Features such as the cyclic nature of the marls and the zoned calcite rims are difficult to explain by tectonic interferences.

The top of lacustrine sequences is characterised by erosive surfaces, indicating a major shift in depositional settings between the successive sedimentary facies. This shift may be caused by tectonism affecting topographic morphology as proposed by Martini and Capezzuoli (2014) for the mixed fluvial clastic deposits and calcareous tufa from the Pianizzoli area (Southern Toscany, Italy). However, in agreement with the conclusion of Van Noten et al. (2013), this study did not find any evidence for significant synsedimentary tectonic activity. Therefore, it is argued that the transition between different facies reflects a shift of the hydrological regime, related to climatic change changes, whereby precipitation patterns changed, causing rainfall to decrease and lakes to dry up (Fig. 13b). The latter would lead to the subaerial exposure of the lake sediments, allowing widespread pedogenesis to take place. The absence of sedimentary features, typically linked to pedogenesis, can be explained due to a fast transition from lacustrine to fluvial deposits, only leading to a limited time for subaerial exposure, which was insufficient for soil formation. Furthermore, it could also be that the pedogenetic features have been eroded. An argument in favour of a gradual change to more arid climatic conditions is the precipitation of palygorskite and authigenic dolomite, which according to Botha and Hughes (1992) reflect diagenesis in an arid regime. However, it is clear that for strengthening the latter argument, the use of other paleoenvironmental proxies (pollen, isotopes, fossils, etc.) should be integrated. Bursts of heavy rainfall may still occur in this overall dry climate, similar to Wadi systems (Matter et al. 2016; Spalletti and Piñol 2005), which would lead to the deposition of fluvial sediments as addressed below.

Shoreline facies

A first coquina lithotype (Type I) is interpreted to reflect shoreline facies, in which mostly intact gastropods are observed, indicating limited transport. These beds were characterised by cross-laminations and were observed in close proximity of laminated marls. Deposition of these gastropod beds is typically linked to lake shorelines, where vast amounts of gastropods lived and were concentrated in thin beds due to wave shoaling (Chinelatto et al. 2018; Fick et al. 2018). These beds are thus interpreted to correspond to paleo-shorelines of the lake systems (Fig. 13).

In addition, the alignment of these shells in planar horizons is an indicator for a sub-horizontal depositional environment, in correspondence with the adjacent sub-horizontal travertines (Fig. 10a, b). Moreover, the proximity of the lacustrine facies and travertine deposits point to a subaquatic setting, in which bioclastic accumulation of gastropods could take place. The gastropods belong to the Hydrobiidae family, supporting the freshwater setting. The proximity of the lacustrine system explains the occurrence of well-cemented gastropod beds along the boundary of the lacustrine and travertine system.

Fluvial facies

Polygenetic conglomerates, tabular sandstones, massive marls, and the second lithotype of coquina accumulations (Type II) are all spatially closely associated with each other and display characteristic features such as erosive channels, cross-lamination, and pebble imbrications. Therefore, these lithologies are grouped in the fluvial facies.

Two types of conglomerate-filled channels were observed, either being simultaneously deposited channels (I) or amalgamated channels (II). The presence of the first might indicate the existence of braided river systems (Amireh et al. 1994; Liébault et al. 2013), while the second indicates that the channel location persisted over a certain time period. In between these conglomeratic channels, massive and non-laminated marls are observed, which are interpreted as alluvial floodplain deposits—part of the river system. The local presence of pebbles within these marls, supporting temporary high-energy and dynamic environmental conditions, indicates that they were deposited in a setting different from that of the laminated marls. In addition, calcite-encrusted reed stems are observed in these marls, especially in proximity of conglomeratic channels. The presence of these calcite encrustations implies that fluids, present in areas adjacent to these river channels, were supersaturated with $CaCO_3$. Therefore, at least a fraction of these waters is assumed to originate from the adjacent travertine system. Similar mechanisms of calcite precipitation on reed stems have been described by Janssen et al. (1999).

Imbrication structures and unidirectional cross-lamination, indicating a paleoflow direction from north to south, generally imply an elevated flow rate in these paleo-rivers. This flow direction is likely controlled by the graben shoulder, forming a topographic high in the north. The diversity of rock units in the provenance area translates into a heterogeneous clast composition, originating from the Menderes Massif (northwest) or the Ophiolite complexes (north). An exception regarding these exotic pebbles are the large and angular travertine boulders, dominantly composed of the sub-horizontal travertine facies. Their size and angularity are the indicators of a proximal provenance area, corresponding to erosion of adjacent travertines.

Tabular sandstones are generally rather thin, but areally extensive lithologies (Fig. 9b). Therefore, they are interpreted to reflect crevasse splays (Fig. 13b). The latter are likely to form during flash floods, caused by sudden and heavy rainfall, typically occurring in dry climates (Amireh et al. 1994; Matter et al. 2016). Ball-and-pillow structures are considered to be the indicators for soft-sediment deformation, caused by tectonic activity after deposition (Fig. 6c). Associated with these tabular sandstones are the second coquina lithotype accumulations, characterised by the presence of cross-laminations and the predominance of crushed gastropod shells (Fig. 9b). The presence of gastropod shells in poorly cemented sediments, such as tabular sandstones, can be explained by gastropods originating from small, isolated pools located in between different river channels (Besacier-Monbertrand et al. 2010; Mtelela et al. 2017). Therefore, they thus imply a different depositional environment as the shoreline facies, which is closely associated with the lacustrine deposits, and dominantly formed in-situ.

The degree of cementation of the fluvial deposits varies strongly in function of the distance from the travertine dome. Polygenetic conglomerates in proximity of the travertine dome are embedded in a strongly cemented matrix, while their distal equivalents are often still unconsolidated and embedded in a calcareous clay matrix. This implies that cementation of the matrix took place after deposition and is eogenetic in origin. It is related to the proximity of the travertine depocentre and percolating carbonate-rich waters. Moreover, the calcite cements of these conglomerates are non-luminescent, similar to calcite cements within the adjacent travertines (Claes et al. 2015). It is thus likely that similar fluids, as the ones causing travertine precipitation, welded together the fluvial lithologies after deposition. This could have happened when travertine vents were (re) activated, allowing carbonate-saturated waters to percolate through proximal conglomerates. In addition, moulds of dissolved clasts are regularly observed in the polygenetic conglomerates, indicating that dissolution took place after cementation. The outlines of these moulds are marked by clay coatings. All of these moulds are partly filled by a later

generation of calcite cement (Fig. 6f). Whether or not these conglomerates are cemented will strongly affect the petrophysical properties of these conglomerates, since these calcite cements can destroy interclast porosity.

Detrital sequences

Since there is no clear evidence for synsedimentary tectonic activity, causing sediment accommodation space to change, the different detrital facies can best be explained by changes of the climate. Increased rainfall would be able to explain both an increased influx of detrital sediments (I) as well as the occurrence of fluvial and lacustrine sediments (II). Cyclic repetition of carbonate and detrital deposits can be attributed to both a decrease in thermal spring activity (I) and a dilution of carbonate-rich water by rainfall (II). It is likely that both mechanisms took place at the same time, however, since no climatological proxies are presented in this paper, it is impossible to differentiate between the two possible mechanisms. It is assumed that lacustrine deposits require a climate with a general abundance of rainfall (perennial rain-dominated system). This allows lake bodies to form, in which thick layers of laminated marls may be deposited. This is in contrast with the fluvial braided river deposits, requiring drier periods with temporary rainfall (seasonal rain-dominated system). The decreased influx of fresh water will cause lake bodies to disappear and succeeded by a braided river system. Temporary bursts of rainfall would in that scenario explain the presence of crevasse splays within the fluvial sediments (Fig. 13).

The first detrital sequence has a limited thickness and is solely characterised by fluvial deposits (Fig. 3). The shift from a carbonate-dominated system to a braided river system requires both an influx of detrital matter, potentially in combination with decreased spring activity. This leads to the deposition of channel conglomerates, consisting of a mixture of fine-grained metamorphic rock fragments and boulder-sized travertine clasts.

The second detrital sequence is characterised by fluvial deposits at the bottom and top, while lacustrine deposits dominate the centre of this sequence (Fig. 5). The onset of this sequence is interpreted to be associated with a gradual increase in rainfall. The latter dilutes thermal spring waters, and thus limits travertine deposition, whilst increases detrital influx through braided river systems. A progressive transition towards a wet climate leads to the formation of lake systems, dilution of waters from the travertine system, and the deposition of lacustrine sediments at the centre of this sequence (Fig. 13). Hereafter, a general shift towards a seasonal rain-dominated system leads again to the deposition of fluvial sediments. The latter are succeeded by new continental carbonate deposits without any influx of detritals, thus requiring a decrease in rainfall and/or an increase in thermal spring activity. The latter is supported by Van Noten et al. (2013) and Claes et al. (2015) who concluded that these carbonates are fed by deep-groundwater expulsion along faults.

The third detrital sequence is characterised by two different subunits, both starting off with fluvial deposits that are gradually replaced by lacustrine sediments (Fig. 5). As a working hypothesis, the interruption of travertine deposition is again associated with the transition towards a rain-dominated climatological setting, initially leading to the deposition of fluvial lithologies. Later on, these fluvial lithologies are gradually replaced by lacustrine sediments, likely implying a change of seasonal to perennial rainfall. The base of the second succession is again dominated by fluvial sediments, which is again hypothesised to reflect a drier climate with periods of heavy rainfall. Similar to the first sequence, these fluvial lithologies are again replaced by lacustrine lithologies, associated with a shift towards a climate with a more continuous surface-water supply.

The fourth and final detrital sequence developed on top of the domal travertines and marks the end of travertine deposition in the Ballık area. The base of this detrital sequence is made of lacustrine sediments, passing into fluvial deposits. The deposition of detrital sediments on travertine strata implies the (partial) submergence of the travertine system, leading to the widespread deposition of lacustrine sediments. The partial submergence is assumed to be associated with a wet climate, in which travertine precipitating fluids are so diluted that widespread travertine formation stops. It could also relate to a change in the hydrological setting whereby the travertine precipitating fluid flow stopped. The top of this sequence is dominated by fluvial lithologies, marking an important climatological shift with the predominance of braided river systems.

Reservoir characteristics

Based on the limited amount of petrophysical measurements, preliminary implications of detrital sediments on a continental carbonate reservoir analogue system can be made. Both fluvial and lacustrine facies are volumetrically most abundant, representing a similar volume as the pure carbonate lithologies in the quarried Ballık study area, at least based on the exposed part of it. However, on a reservoir scale, it is likely that the lacustrine and fluvial facies are volumetrically more abundant than the pure carbonate lithologies. The latter are likely to form domal structures in the vicinity of faults, while the accommodation space in between these domes would be filled with detrital sediments. 2D-porosity estimations for lacustrine sediments show a great variability. Furthermore, framework stabilizing cements are absent in the lacustrine sediments, making the porosity within these sediments vulnerable to compaction. Fluvial conglomerates can initially form fair reservoir units (Leverson,

1954). However, in close proximity of the travertines, they are prone to cementation due to percolating carbonate-rich waters. The latter leads to pore-blocking cements that diminish porosity and permeability.

With emphasis on a reservoir analogue, marly lacustrine deposits are likely to develop in between travertine structures, lowering the interconnectivity between superimposed travertine successions. In case of complete flooding of travertine structures, marls can be deposited on top of travertine systems, lowering vertical connectivity between successive travertine sequences. Lacustrine sediments, covering travertine structures, are thus likely to lead to the development of potential seals. The fluvial facies is more likely to interconnect different parts of a reservoir, either by improving its lateral continuity or by vertical erosion and amalgamation. However, it has to be kept in mind that the fluvial facies is prone to the development of pore-blocking cements, decreasing porosity and especially permeability.

The shoreline facies does not represent a significant volume (< 1%) in the reservoir analogue. Moreover, the dimensions of these sediment bodies are often limited, reducing their possible influence on a reservoir scale.

Conclusion

Several detrital sequences are observed proximal to the travertine deposits of the Ballık area. They are made up of five detrital lithologies, which are described in this study both macroscopically and microscopically. Each of these lithologies can be assigned to a specific sedimentary facies, mainly based on their sedimentary and depositional characteristics. Three different detrital facies are identified within a 500 m lateral reach of the quarried travertine system, namely the lacustrine, the shoreline, and the fluvial facies. Therefore, it has to be kept in mind that the true dimensions of these detrital facies might be significantly larger on a reservoir scale then what is reported in this study.

1. The Quaternary deposits in the Ballık area are generally characterised by either detrital or continental carbonate deposits, which can either dominate the sedimentary record or occur simultaneously next to one another. Both climate and tectonics can affect the abundance of either type of deposit. Even though major tectonic events may lead to the creation of topographic lows, allowing lake bodies to form, no arguments for major synsedimentary deformation have been observed in the study area. In addition, most known tectonic activities in the Ballik area postdate sediment deposition according to Van Noten et al. (2013). Therefore—though an external tectonic control cannot be completely excluded—changes in climate and precipitation patterns are a more likely mechanisms to explain (I) cyclicities in the sedimentary record and (II) the increased influx of detrital sediments. Furthermore, a decrease in thermal spring activity might also affect travertine formation. A combination of both mechanisms can thus explain the dominance of either pure carbonate or detrital sediments on a given location (Fig. 13).
2. Lacustrine sediments correspond to periods dominated by continuous rainfall, where seasonal variations lead to varve-like deposits. Furthermore, shorelines of these lake systems are characterised by coquina deposits (Fig. 13). The transition to non-continuous rainfall periods results in soil formation to take place in these lacustrine sediments, corresponding to the formation of authigenic palygorskite and dolomite. Associated with this transition, towards a non-continuous rainfall period, is the deposition of fluvial lithologies.
3. The mixed clastic–carbonate system of the Ballık area shows that clastic sediments can strongly affect reservoir architecture. Thick lacustrine sediments were observed in between and on top of carbonate lithologies and are likely to become impermeable due to compaction during burial. On a reservoir scale, these lacustrine sediments might thus lead to the compartmentalization of individual carbonate build-up structures as such. Fluvial sediments might initially act as fluid pathways; however, in the Ballık area, they were observed to be completely cemented in proximity of the travertine system. The latter thus destroys both permeability and porosity of these conglomeratic beds, making it unlikely they will act as fluid pathways within a reservoir system.

Acknowledgements Special gratitude goes to Johanna van Daele (KU Leuven) for the SEM images and to Thomas Neubauer (Justus Liebig University) for the classification of the gastropod as Hydrobiidae. We would like to thank Herman Nijs (KU Leuven) for the preparation of the thin sections. We are also grateful to Nancy Weyns (KU Leuven) and Ria Brepoels (KU Leuven) for the help with the mineralogical measurements. Furthermore, the guidance of Mehmet Özkul (Pamukkale University) helped us to carry out the field campaign successfully. Finally, we would still like to thank the Editor of IJES and the reviewer for her constructive and detailed feedback on this paper.

References

Alçiçek MC, Brogi A, Capezzuoli E, Liotta D, Meccheri M (2013) Superimposed basin formation during the Neogene-Quaternary extensional tectonics in SW-Anatolia (Turkey): insights from the kinematics of the Dinar Fault Zone. Tectonophysics 608:713–727

Alçiçek H, Bülbül A, Yavuzer I, Alçiçek MC (2019) Origin and evolution of the thermal waters from the Pamukkale Geothermal Field (Denizli Basin, SW Anatolia, Turkey): Insights from hydrogeochemistry and geothermometry. J Volcanol Geoth Res 372:48–70

Amireh BS, Schneider W, Abed AM (1994) Evolving fluvial-transitional-marine deposition through the Cambrian sequence of Jordan. Sediment Geol 89(1–2):65–90

Bayliss P, Erd DC, Mrose ME, Sabina AP, Smith DK (1986) Mineral powder diffraction file. search manual. International Centre for Diffraction Data, Swarthmore, USA, p 467

Bear J (1972) Dynamics of fluids in porous media. American Elsevier Publishing Company, New York, p 764

Beltrão RLC, Sombra CL, Lage ACVM, Fagundes Netto JR, Henriques CCD (2009) Challenges and new technologies for the development of pre-salt cluster, Santos Basin, Brazil. Offshore Technology Conference, Houston, Texas, USA, pp 587–597

Besacier-Monbertrand AL, Paillex A, Castella E (2010) Alien aquatic macroinvertebrates along the lateral dimension of a large floodplain. Biol Invasions 12(7):2219–2231

Boehrer B, Schultze M (2008) Stratification of lakes. Rev Geophys 46(2):210–236

Boggs S, Krinsley DH (2006) Application of cathodoluminescence imaging to the study of sedimentary rocks. Cambridge University Press, Camebridge, p 165

Botha GA, Hughes JC (1992) Pedogenic palygorskite and dolomite in a late Neogene sedimentary succession, northwestern Transvaal, South Africa. Geoderma 53:139–154

Bozkurt E (2001) Neotectonic of Turkey-a synthesis. Geodin Acta 14:3–30

Bozkurt E (2003) Origin of NE-trending basins in western Turkey. Geodin Acta 16:61–81

Capezzuoli E, Ruggieri G, Rimondi V, Brogi A, Liotta D, Alçiçek H, Bülbül A, Gandin A, Meccheri M, Shen CC, Baykara MO (2018) Calcite veining and feeding conduits in a hydrothermal system: Insights from a natural section across the Pleistocene Gölemezli travertine depositional system (western Anatolia, Turkey). Sediemnt Geol 364:180–203

Carnicelli S, Benvenuti M, Andreucci S, Ciampalini R (2015) Late Pleistocene relic Ultisols and Alfisols in an alluvial fan complex in coastal Tuscany. Quatern Int 376:163–172

Chinelatto GF, Vidal AC, Kuroda MC, Basilici G (2018) A taphofacies model for coquina sedimentation in lakes (Lower Cretaceous, Morro de Chaves Formation, NE Brazil). Cretac Res 85(5):1–19

Claes H, Soete J, Van Noten K, El Desouky H, Marques Erthal M, Vanhaecke F, Özkul M, Swennen R (2015) Sedimentology, three-dimensional geobody reconstruction and carbon dioxide origin of Pleistocene travertine deposits in the Ballık area (south-west Turkey). Sedimentology 62:1408–1445

Croci A, Della Porta G, Capezzuoli E (2016) Depositional architecture of a mixed travertine-terrigenous system in a fault-controlled continental extensional basin (Messinian, Southern Tuscany, Central Italy). Sed Geol 332:13–39

Delicado D, Machordom A, Ramos MA (2013) Living on the mountains: Patterns and causes of diversification in the springsnail subgenus Pseudamnicola (Corrosella) (Mollusca: Caenogastropoda: Hydrobiidae). Mol Phylogenet Evol 68(3):387–397

El Desouky H, Soete J, Claes H, Özkul M, Vanhaecke F, Swennen R (2015) Novel applications of fluid inclusions and isotope geochemistry in unravelling the genesis of fossil travertine systems. Sedimentology 62:27–56

Fick C, Toldo EE Jr, Puhl E (2018) Shell concentration dynamics driven by wave motion in flume experiments: insights for coquina facies from lake-margin settings. Sed Geol 375:98–114

Gawthorpe RL, Leeder MR (2000) Tectono-sedimentary evolution of active extensional basins. Basin Res 12:195–218

Gawthorpe RL, Fraser AJ, Collier REL (1994) Sequence stratigraphy in active extensional basins: Implications for the interpretation of ancient basin-fills. Mar Pet Geol 11:642–658

Gierlowski-Kordesch E, Finkelstein DB, Holland T, J.J., Kallini, K.D. (2013) Carbonate lake deposits associated with distal siliciclastic perennial-river systems. J Sediment Res 83(12):1114–1129

Jackson ML (1973) Soil Chemical Analysis. Prentice Hall of India Pvt. Ltd., New Delhi, p 498

Janssens A, Swennen R, Podoor N, Keppens E (1999) Biological and diagenetic influence in recent and fossil tufa deposits from Belgium. Sed Geol 126:75–95

Khatib S, Rochette P, Alçiçek MC, Lebatard AE, Saos T (2014) Stratigraphic, sedimentologic and paleomagnetic study of the Kocabas travertines, Denizli Basin, Anatolia. Anthropologie 118:16–33

Lebatard AE, Alçiçek MC, Rochette P, Khatib S, Vialet A, Boulbes N, Bourlès DL, Demory F, Guipert G, Mayda S, Titov VV, Vidal L, de Lumley H (2014) Dating the Homo erectus bearing travertine from Kocabaş (Denizli, Turkey) at least 1.1 Ma. Earth Planet Sci Lett 390:8–14

Leverson AI (1954) Geology of Petroleum: San Francisco. W.H. Freeman and Co., New York, p 703

Liébault F, Lallias-Tacon S, Cassel M, Talaska N (2013) Long profile responses of alpine braided rivers in SE France. River Res Appl 29(10):1253–1266

Ma J, Wu C, Wang Y, Wang J, Fang Y, Zhu W, Zhai L, Zhou T (2017) Paleoenvironmental reconstruction of a saline lake in the Tertiary: evidence from aragonite laminae in the northern Tibet Plateau. Sed Geol 353:1–12

Martini I, Capezzuoli E (2014) Interdigitated fluvial clastic deposits and calcareous tufa testifying an uplift of the catchment area: an example from the Pianizzoli area (southern Tuscany, Italy). Sed Geol 299:60–73

Matter A, Mahjoub A, Neubert E, Preusser F, Schwalb A, Szidat S, Wulf G (2016) Reactivation of the Pleistocene trans-Arabian Wadi ad Dawasir fluvial system (Saudi Arabia) during the Holocene humid phase. Geomorphology 270:88–101

Moore DM, Reynolds RC (1997) X-Ray Diffraction and the Identification and Analysis of Clay Minerals, 2nd edn. Oxford University Press, New York, p 378

Mors RA, Astini RA, Gomez FJ (2019) Coexisting active travertines and tufas in the southeastern border of the Puna plateau. Sed Geol 389:200–217

Mtelela C, Roberts EM, Hilbert-Wolf HL, Downie R, Hendrix MS, O'Conner PM, Stevens NJ (2017) Sedimentology and paleoenvironments of a new fossiliferous late Miocene-Pliocene sedimentary succession in the Rukwa Rift Basin, Tanzania. J Afr Earth Sc 129:260–281

Muniz MC, Bosence DWJ (2015) Pre-Salt microbialites from the Campos Basin (offshore Brazil): image log facies, facies model and cyclicity in lacustrine carbonates. Geolog Soc Lond Spec Publ 418:221–242

Nash MC, Opdyke BN, Wu Z, Xu H, Trafford JM (2013) Simple X-ray diffraction to identify MG calcite, dolomite and magnesite in tropical coralline algae and assess peak assymentry. J Sediment Res 83:1084–1098

Özkul M, Kele S, Gökgöz A, Shen CC, Jones B, Baykara MO, Fórizs I, Németh T, Chang YW, Alçiçek MC (2013) Comparison of the Quaternary travertine sites in the Denizli extensional basin based on their depositional and geochemical data. Sed Geol 294:179–204

Rausch L, Alçiçek H, Vialet A, Boulbes N, Mayda S, Titov VV, Stoica M, Charbonier S, Abels HA, Tesakov AS, Moigne A-M, Andrieu-Ponel V, de Franceschi D, Wesselingh FP, Alçiçek MC (2019) An integrated reconstruction of the early Pleistocene palaeoenvironment of Homo erectus in Denizli Basin (Turkey). Geobios 57:77–95

Renaut RW, Owen RB, Jones B, Tiercelin JJ, Tarits C, Ego JK, Konhauser KO (2012) Impact of lake-level changes on the formation

of thermogene travertine in continental rifts: evidence from Lake Bogoria. Kenya Rift Valley Sedimentol 60(2):424–468

Rodas M, Luque FJ, Mas R, Garzon MG (1994) Calcretes, palycretes and silcretes in the Paleogene detrital sediments of the Duero and Tajo Basins, Central Spain. Clay Miner 29:273–285

Rodriguez-Blanco JD, Shaw S, Benning LG (2015) A route for the direct crystallization of dolomite. Am Miner 100:1172–1181

Ronduit N (2007) JMicroVision: un logiciel d'analyse d'images pétrographiques polyvalent. PhD thesis presented at the Faculty of Sciences of the University of Genève to obtain the degree of Doctor in Science. Thesis n, 3830

Serck CS, Braathen A (2019) Extensional fault and fold growth: Impact on accommodation evolution and sedimentary infill. Basin Res 31(5):967–990

Soete J, Kleipool L, Claes H, Claes S, Hamaekers H, Kele S, Özkul M, Foubert A, Reijmer J, Swennen R (2015) Acoustic properties in travertines and their relation to porosity and pore types. Mar Pet Geol 59:320–335

Sözbilir H (2002) Revised stratigraphy and facies analysis of palaeocene-eocene supra-allochthonous sediments (Denizli, SW Turkey) and their tectonic significance. Turkish J Earth Sci 11:87–112

Spalletti LA, Piñol FC (2005) From alluvial fan to playa: an upper jurassic ephemeral fluvial system, Neuquén Basin. Argent Gondwana Res 8(3):363–383

ten Veen JH, Boulton SJ, Alçiçek MC (2009) From palaeotectonics to neotectonics in the Neotethys realm: the importance of kinematic decoupling and inherited structural grain in SW Anatolia (Turkey). Tectonophysics 473:261–281

Toker E, Kayseri-Özer MS, Özkul M, Kele S (2015) Depositional system and palaeoclimatic interpretations of Middle to Late Pleistocene travertines: Kocabaş, Denizli, south-west Turkey. Sedimentology 62(5):1360–1383

Valero-Garcés B, Morellón M, Moreno A, Corella JP, Martín-Puertas C, Barreiro F, Pérez A, Giralt S, Mata-Campo MP (2014) Lacustrine carbonates of Iberian Karst Lakes: sources, processes and depositional environments. Sed Geol 299:1–19

Van Noten K, Claes H, Soete J, Foubert A, Özkul M, Swennen R (2013) Fracture networks and strike-slip deformation along reactivated normal faults in Quaternary travertine deposits, Denizli Basin, western Turkey. Tectonophysics 588:154–170

Van Noten K, Baykara O, Topal S, Claes H, Ozkul M, Swennen R, Aratman C (2019) Pleistocene-Holocene tectonic reconstruction of the Ballık travertine (Denizli Graben, SW Turkey): (De)formation of large travertine geobodies at intersecting grabens. J Struct Geol 118:114–134

Virgone A, Broucke O, Held AE, Lopez B, Seard C, Camoin G, Swennen R, Foubert A, Rouchy JM, Pabian-Goyheneche C, Guo L (2013) Contintental carbonates reservoirs: the importance of analogues to understand presalt discoveries. International Petroleum Technology Conference, Beijing, China, pp 4439–4447.

Walk J, Stauch G, Bartz M, Brückner H, Lehmkuhl F (2019) Geomorphology of the coastal alluvial fan complex Guanillos, northern Chile. J Maps 15:436–447

Welton JE (1984) SEM petrology atlas. American Association of Petroleum Geologists, Oklahoma, p 237p

Westaway R, Guillou H, Yurtmen S, Demir T, Scaillet S, Rowbotham G (2005) Constraints on the timing and regional conditions at the start of the present phase of crustal extension in western Turkey, from observations in and around the Denizli region. Geodin Acta 18(3–4):209–238

Xie Q, Chen T, Zhou H, Xu X, Xu H, Ji J, Lu H, Balsam W (2013) Mechanism of palygorskite formation in the Red Clay Formation on the Chinese Loess Plateau, northwest China. Geoderma 192:39–49

Zolitschka B, Francus P, Ojala AEK, Schimmelmann A (2015) Varves in lake sediments: a review. Quat Sci Rev 117:1–41